TU WIEN

A New Efficient Real-Time Global Tone Mapping Method

by

Georg Spielmann

Schwarzgruberg. 10 A-1100 Vienna

A Thesis Submitted at the Institute of Computer Graphics and Algorithms of the Technical University of Vienna in Partial Fulfillment of the Requirements for the Degree

MASTER OF SCIENCE

Supervised by:

Werner Purgathofer
Head of the Institute of Computer Graphics and Algorithms, Technical University Vienna, Austria

László Neumann
Professor at the University of Girona, Spain

Vienna, Austria

June, 2006

ABSTRACT

A New Efficient Real-Time Global Tone Mapping Method

by

Georg Spielmann

In computer graphics, visualization, digital imaging and specially in digital photography, tone mapping plays an important role. The contrast of an image is finite and display device dependent. It is typically around 4-6 stops according to photographical tradition in log2 scale. The contrast of the original scene however is often significantly greater than that so that the bright or dark parts of the scene will have no details in the image. A classical photography pipeline doesn't manipulate the image after an automatic exposure.

In this work we give an overview of color science, human vision and display devices. We present known global tone mapping methods and some efficient adaptive HDR methods.

The main focus of the work is to find the optimum contrast window for global

tone mapping and to decide if there are better global and local mapping methods than the widespread mean value mapping. This work deals with the generalization of the minimal information loss method and the empirical search for optimal parameter combinations for the method.

It is combined, in an innovative way, with the max(r,g,b) function (instead of luminance) introduced in incident light metering for computer graphics, or quasi-irradiance principle. These two methods yield visually pleasant results high contrast images, e.g. for the always critical back light or images containing exterior and interior parts simultaneously. Since the method works in real time, after further improvements it could be easily included in Digital Cameras.

KURZFASSUNG

A New Efficient Real-Time Global Tone Mapping Method

by

Georg Spielmann

In der Computer Graphik, Visualisierung und vor allem in der digitalen Photographie spielt Tone Mapping eine wichtige Rolle. Der Kontrast eines Bildes ist endlich und abhängig vom Ausgabegerät. Normalerweise ist er zwischen 4-6 auf einer log2 Skala. Der Kontrast der realen Szene ist aber meistens bedeutend höher, so dass sehr helle und sehr dunkle Teile des Bildes Detailarm dargestellt werden.

In dieser Arbeit wird ein Überblick über Farbtheorie, das menschliche sehen und ber verschiedene Ausgabegeräte gegeben. Es werden bekannte globale Tone Mapping Methoden beschrieben und einige effiziente lokale Methoden.

Das Hauptaugenmerk dieser Arbeit ist es das optimale Kontrastfenster für Globales Tone Mapping zu finden und festzustellen ob es bessere globale und lokale Mapping Methoden als das weit verbreitete Mean Value Mapping gibt. In der Arbeit wird

eine Verallgemeinerung der Minimal Information Loss Methode beschrieben und es wird empirisch nach den besten Parameterkombinationen fr diese Methode gesucht. Diese Methode ist in einer innovativen Weise mit dem max(r,g,b) Prinzip kombiniert das f*ü*r Incident Light Metering vorgestellt wurde. Diese Kombination erzeugt visuell ansprechende Bilder f*ü*r Szenen mit Gegenlicht oder Szenen mit Informationen aus dem Inneren und dem *Ä*usseren. Da es sich um eine Echtzeit Methode handelt k*ö*nnte sie, nach weiterer Entwicklung, in Digital Kameras eingebaut werden.

Acknowledgments

My very special thanks go to Prof. László Neumann from the Universidad de Girona which was so kind to receive me in Girona and spend a lot of his time with me to explain me his innovative techniques or just to have a cup of coffee and a good talk.

I would also like to thank Prof. Werner Purgathofer, the head of the Computer Graphics institute of the Technical University of Vienna for giving me the possibility and encouraging me to write parts of this work in Spain and always having time for discussing my problems.

Contents

Chapter 1
Introduction

To capture the physical appearance of real and modelled scenes is one of the main goals in digital photography as well as in realistic image synthesis. To reach this goal the simulation of the human visual system is intended. The human eye can distinguish reliably in a range from below starlight to sunlight ($10^{-6}cd/m^2$ to $10^6cd/m^2$).Hence a problem which occurs trying to simulate the human visual system is that most of the time the visual range of light energy in the scene differs by far the one of the output device. In that case a scene is said to have high dynamic range. Images with very large dynamic range have become common and therefore new file formats and new output devices have been developed. The RGBE [38] format stores the luminance values apart from the 3 color channels. It is still almost impossible to reproduce those values correctly on a standard output device (like a CRT monitor for example). Therefore one must think of other possibilities to reproduce the original scene on the dynamic range of the given display device. Transformations that preserve the appearance of the scene, so called Tone Mapping methods, can be used. The first tone mapping operator was introduced by Tumblin and Rushmeier [34]. Even if the current research seems to be more interested in High Dynamic Range Imaging and adaptive tone mapping methods, most of the light management in nowadays digital

photo cameras is still handled by a simple global tone mapping operator. This is due to the fact that adaptive methods are still way to complex to calculate in real time. This is why we present an evolved version of the Minimal Information Loss method [20] which represents a, by far, more pleasant result to the human eye then the widely used Average Light method. Hence, we will not try to simulate every behavior of the human visual system, since that would demand highly complicated adaptive methods, but instead give an easy, robust, almost instinctive method which could be used for real time applications like games or in any digital camera to produce high quality pictures.

Chapter 2
Color Science and Human Vision

Some knowledge of color science and the human visual system is necessary to understand the tone mapping method presented in this work. Color science has been influenced by philosophers, artists, physicists, chemists, psychologists, neurologists, graphical designers and computer scientists. Obviously there is a huge amount of research in this field of study and only a small elementary part will be covered in this thesis. Basically the term color describes at least 3 different things:

- Object properties (green grass)
- Characteristic of light rays (grass reflects green light)
- A sensation of the human perceptory system (we perceive grass to be green)

The way we perceive an object depends on these 3 factors. Clearly we cannot see without light. But the perception of object also changes under different lighting conditions. For example people look at color of cloth in natural daylight in front of stores to have a good impression before buying them. The properties of the object itself are also fundamental. Grass is green, some objects are red, some are blue etc. And finally the human perception plays a big role. It is quite a challenge to describe the sensation of color, in fact it is impossible. Nevertheless we can tell if a color looks the same or similar to another color, but this is not a description of color. Methods

exist to measure colors and light which we will describe briefly in the following part. First we will give an overview of photometry and radiometry, then introduce some of the anatomy of the human eye and some characteristics of the human visual system and finally give a basic overview of colorimetry.

2.1 About Light

According to *The Concise Oxford English Dictionary, (5th Edition, 1964)*, light is:

1. The natural agent that stimulates the sense of sight.

2. Medium or condition of space in which sight is possible

Even in physics the true nature of light isn't totaly clarified. Although the true nature of light is not clear, in this chapter we will only deal with the question how light is measured.

Light is *electromagnetic radiation.*The visible range of the human visual system is only a small fraction of the entire electromagnetic spectrum (see fig. 2.1). Depending on the frequency the spectrum contains very low frequency radio waves, microwaves, infrared, visible light, ultraviolet light, x-rays and ultraenergetic gamma rays. Special equipment is necessary to detect the parts of the spectrum which are not in the visible range.

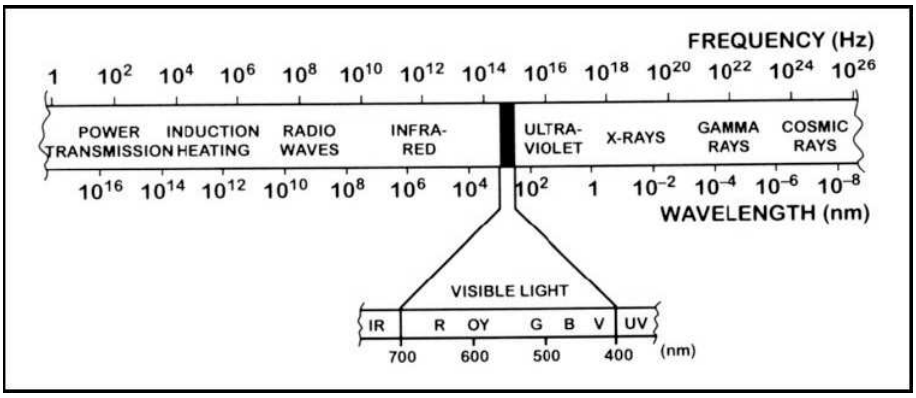

Figure 2.1 Electromagnetic Spectrum

2.2 Photometry

Photometry is the science of measuring visible light in units that are weighted according to the sensitivity of the human eye. It is a quantitative science based on a statistical model of the human visual response to light. The sensitivity of the human eye to light varies with wavelength. We see light of different wavelengths as a continuum of colors ranging through the visible spectrum: $650nm$ is red, $540nm$ is green, $450nm$ is blue, and so on. The sensitivity of the human eye to light varies with wavelength. A light source with a radiance of one $watt/m2 - steradian$ of green light, for example, appears much brighter than the same source with a radiance of one $watt/m2 - steradian$ of red or blue light. In photometry, we do not measure watts of radiant energy. Rather, we attempt to measure the subjective impression produced by stimulating the human eye-brain visual system with radiant energy [2].

In 1924, the Commission Internationale dEclairage (International Commission on Illumination, or CIE) asked over one hundred observers to visually match the

"brightness" of monochromatic light sources with different wavelengths under controlled conditions. The statistical result shows the photopic luminous efficiency of the human visual system as a function of wavelength. It provides a weighting function that can be used to convert radiometric into photometric measurements. Photometric theory does not address how we perceive colors. The light being measured can be monochromatic or a combination or continuum of wavelengths; the eyes response is determined by the CIE weighting function [2].

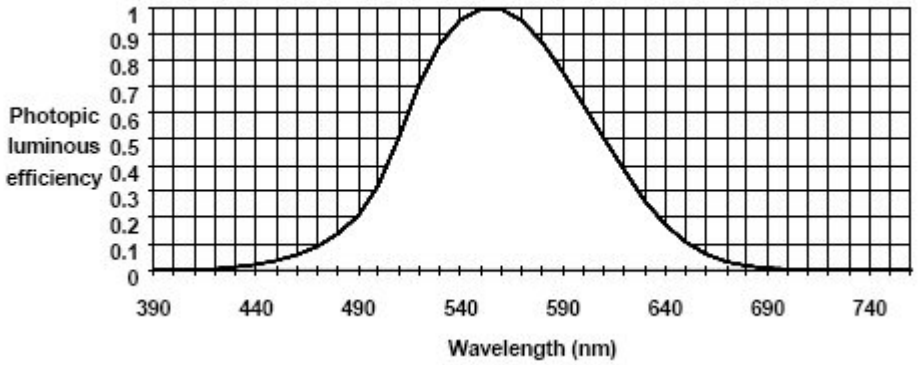

Figure 2.2 CIE Photometric Curve, [2]

The difference between photometry and radiometry are the units of measurements and that photometry takes the visible spectrum (fig. 2.2) into account.

2.3 Radiometry

Radiometry is the science of measuring light in any portion of the electromagnetic spectrum. In practice, the term is usually limited to the measurement of infrared, visible, and ultraviolet light using optical instruments [2]. Light is *radiant energy*

transported through space by electromagnetic radiation. Radiant energy (denoted as Q) is measured in *joules*. A light source like the sun emits electromagnetic radiation almost throughout the whole electromagnetic spectrum, from radio to gamma rays. A single-wavelength laser (stands for **L**ight **A**mplification by **S**timulated **E**mission of **R**adiation), on the other hand, is a monochromatic source, it emits at one specific wavelength only.

Spectral radiant energy is the amount of radiant energy per unit wavelength interval at wavelength λ. It is defined as:

$$Q_\lambda = dQ/d\lambda \tag{2.1}$$

The units are *joules per nanometer*.

Radiant power is the "time rate of flow of radiant energy", or *radiant flux*. It is defined as:

$$\Phi = dQ/dt \tag{2.2}$$

Where Q is radiant energy and t is time. The units are *joules per seconds* or *watts*.

Spectral Radiant Flux (or spectral radiant power) is radiant flux per unit wavelength interval at wavelength λ, defined as:

$$\Phi_\lambda = d\Phi/d\lambda \tag{2.3}$$

measured in *watts per nanometer*

Radiant flux density is radiant flux per unit area at a point on a surface. The flux can be arriving at the surface, in which case the radiant flux density is referred to as *irradiance*, or the flux can be leaving the surface due to emission or reflection. The radiant flux density is then referred to as *radiant exitance*.

Irradiance is defined as:

$$E = d\Phi/dA \tag{2.4}$$

where Φ is the radiant flux arriving at the point and dA is the differential area surrounding the point.

Radiant exitance is defined as:

$$M = d\Phi/dA \tag{2.5}$$

where Φ is the radiant flux leaving the point and dA is the differential area surrounding the point. Accordingly we can define *spectral radiant flux density*. Spectral irradiance $E_\lambda = dE/D\lambda$ and spectral radiant exitance $M_\lambda = dE/D\lambda$. Spectral radiant flux density is measured in watts per square meter per nanometer.

If we think of visualizing radiance, we'll have to imagine a ray of light arriving or leaving a point on a surface in a given direction. Then the radiance is the infinitesimal amount of radiant flux contained in this ray. Formally we would have to think of ray being an infinitesimally narrow cone with its apex at a point on a surface. This cone has a differential solid angle $d\omega$ measured in steradians. We must also note that

Figure 2.3 Irradiance and Radiant exitance, [2]

the ray is intersecting the surface at an angle. If the area of intersection with the surface has a differential cross-sectional area dA, the cross-sectional area of the ray is $dA\cos\Theta$, where Θ is the angle between the ray and the surface normal [2]. The definition of Radiance is then:

$$L = \frac{d^2\Phi}{\cos\Theta dA d\omega} \tag{2.6}$$

where Φ is the radiant flux, dA is the differential area surrounding the point, $d\omega$ is the differential solid angle of the elemental cone, and Θ is the angle between the ray and the surface normal n at the point. Radiance is measured in watts per square meter per steradian. Spectral radiance L_λ is defined accordingly.

2.4 Human Vision

The human visual system (HVS) is by far the most data-intensive sense. Approximately 80% of all input that the human gather with his 5 senses is visual. The principal sensory organ of the human visual system is of course the eye. Although

only the exterior parts of the HVS are reasonably well understood, these are those of interest to color science.

2.4.1 The Visual System

The visual center is situated in the brain. The visual cortex is located at the rear of the scull. The exact functions of the inner brain regions is not entirely clear.

The Eye

The eye consists of: *cornea, pupil, lens, aqueous humour, vitreous body* and *retina*. More to the anatomy of the eye concerning color vision can be read in [40] and [16].

The seen inverted image is focused on the retina. The retina is a light-sensitive tissue. There are two important elements on the retina: *the photoreceptor* and *the fovea*. The fovea is the part of the eye where vision is the most acute. There are 2 different types of photoreceptors in the retina: *rods* and *cons*. In the fovea the density of cones is higher then outside the fovea. That is why images focused on the fovea are resolved very good. The rod and cone systems are sensitive to light with wavelengths from about $400nm$ to $700nm$. The rods have their peak sensitivity at approximately $505nm$. Spectral sensitivity of the composite cone system peaks at approximately $555nm$ [14]. The cons are responsible for color seeing. There are 3 different types of cons in the eye. One type is slightly different from the two others. It

is most responsive to light perceived as violet with wavelengths around $420nm$. These are the so called short-wavelength cones or S-cones. They are also called blue cons which could be a little bit misleading. The other two types of cones are as well more similar genetically as chemically and as in their response. Both types are sensitive to greenish light. One of this cones, the long-wavelength or L-cones or red cones, are most sensitive to a wavelength around $564nm$ which corresponds to a yellowish-green. The other ones are the middle-wavelength cones or M cones or green cones. They have a maximal response at around $534nm$ which we perceive as green.

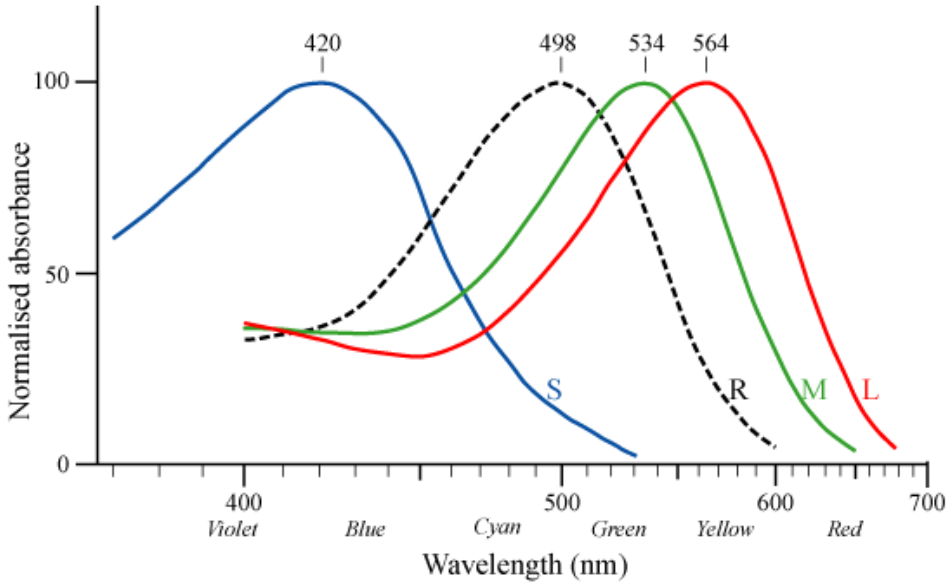

Figure 2.4 Cone and Rod responses

We differ between 3 types of luminance ranges: *scotopic, mesopic* and *photopic*. The rods are extremely sensitive to light and provide achromatic vision at scotopic

levels of illumination raging from 10^{-6} to $10cd/m^2$. The cones are less sensitive than the rods, but provide color vision at photopic levels of illumination in the range of 0.01 to $10^8 cd/m^2$. At light levels from 0.01 to $10cd/m^2$ both the rod and cone systems are active. This is known as the mesopic range [14]. See fig. 2.5

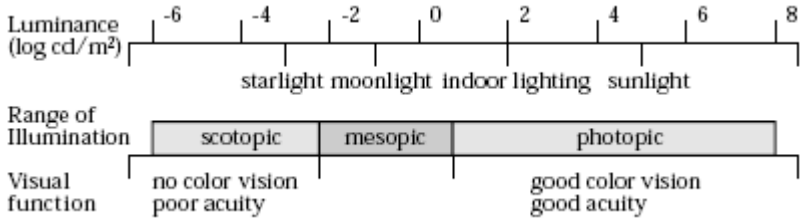

Figure 2.5 The Luminance Range, [14]

2.4.2 Visual Adaptation

The human visual system works over a big range of light levels as the lighting in a scene changes from a dark starlight night to a bright sunny day. Visual adaptation is the process where the human visual system adjusts itself to the actual radiant energy under the current viewing conditions [16]. This adaptation is a result of the coordinated actions of mechanical, photochemical and neural processes in the human visual system. It involves the pupil, the rod and cone systems, bleaching and regeneration of receptor photo-pigments and changes in neural processing. By using these elements the human visual system is able to work over a luminance range of approximately 14 log units. The modifications of the pupil in diameter according to the changes in luminance produces about a log unit change in retinal luminance. This small change

does not allow the pupil action to be sufficient to completely account for visual adaptation [31].

If a photon is captured by one of the receptors within the visual range, the so called *bleaching* is triggered, which is a complex sequence of reactions. At high light intensities, the action of light depletes the photosensitive pigments in the rods and cones at a faster rate than chemical processes can restore them. This makes the receptors less sensitive to light. This process is known as *pigment bleaching* [14]. The neural response produced by a photoreceptor cell depends on chemical reactions produced by the action of light on the cell's photo-pigments. The cell's response to light is limited by the maximum rate and intensity of these chemical reactions. If the reactions are occurring near their maximum levels, and the amount of light striking the photo-pigments is increased, the cell may not be able to fully signal the increase. This situation is known as *saturation*. The result of saturation is *response compression*: above a certain level incremental increases in light intensity will produce smaller and smaller changes in the cell's response rate [14]. The rods and cone system is connected trough a network of neurons in the retina to ganglion cells whose axons form the optic nerve. On this level an adaptive process that adjusts the base activity and gains of the early visual system to mitigate the effects of response compression in the photoreceptors, takes place. A *multiplicative process* adjusts the gain of the system by

effectively scaling the input by a constant related to the background luminance. This process acts very rapidly and accounts for changes in sensitivity over the first few seconds of adaptation. A slower acting *subtractive process* reduces the base level of activity in the system caused by a constant background. This process accounts for the slow improvement in sensitivity measured over minutes of adaptation [14]. Ferwerda used the knowledge of these mechanisms in his psychophysical experiments measuring the changes in visual function that accompany adaptation. The adaptation effects are measured in threshold experiments.

To determine the absolute threshold the screen is made dark. To determine the contrast threshold a large region of the screen is illuminated to a particular background luminance level. Before testing begins, the observer fixates the center of the screen until they are completely adapted to the background level. On each trial a disk of light is flashed near the center of fixation for a few hundred milliseconds. The observer reports whether they see the disk or not. If the disk is not seen its intensity is increased on the next trial. If it is seen, its intensity is decreased. In this way, the detection threshold for the target disk against the background is measured [14].

These curves are known as threshold-vs-intensity functions (TVI). At luminance levels below about $-4 log cd/m2$, the rod curve flattens to a horizontal asymptote. This indicates that the luminance of the background has little effect on the threshold which approaches the limit for detecting a stimulus in the dark. At levels above $2 log cd/m2$

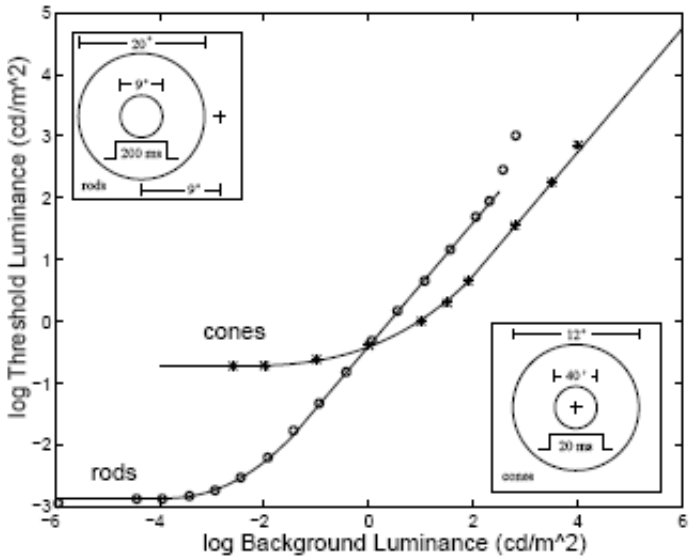

Figure 2.6 A psychophysical model of detection thresholds over the full range of vision,[14]

the curve approaches a vertical asymptote. This indicates that the rod system is being overloaded by the background luminance with the result that no amount of luminance difference between the background and target will allow detection [14]. Over a wide range of background luminance 3.5 log units of background luminance, the size of the threshold increment increases in proportion to the background luminance making the functions linear on a log-log scale. This linear relationship $\Delta L = kL$ is known as *Weber's law* and indicates that the visual system has constant contrast sensitivity since the Weber contrast $\Delta L/L$ is constant over this range [22].

The rod and cone system differ greatly in sensitivity and operate over different luminance ranges which can be seen in figure 2.7. Figure 2.7 (a) shows the visual

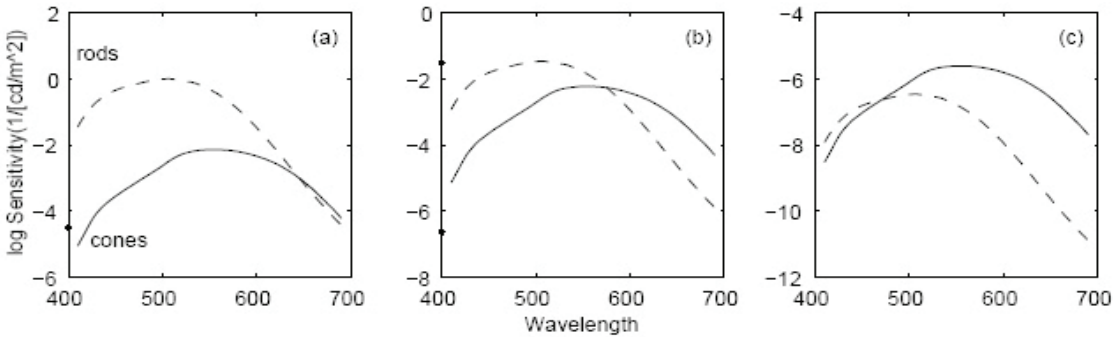

Figure 2.7 Changes in the spectral sensitivity of the visual system at (a) scotopic, (b) mesopic, and (c) photopic illumination levels, [14]

system's spectral sensitivity at scotopic levels. At these levels detection is dominated by the rod system. Absolute sensitivity is quite high, but since the rod system is achromatic, color will not be apparent. Figure 2.7 (b) shows spectral sensitivity at mesopic levels. Here the rod and cone systems are nearly equal in absolute sensitivity. Figure 2.7 (c) shows the visual system's spectral sensitivity at photopic levels. At these levels detection is dominated by the cone system. Absolute sensitivity has dropped considerably, but due to the trichromatic nature of the cone system, colors will now be seen. [14]

Figure 2.8 shows the luminous efficiency function as surfaces positioned with respect to the rod and cone system threshold sensitivities at different luminance levels [14]. It shows how the spectral sensitivity of the HVS changes under different luminance levels and which system is dominant at a particular level.

This model of the changes in spectral sensitivity with changing luminance levels can account for a number of different color appearance phenomena observed over the sco-

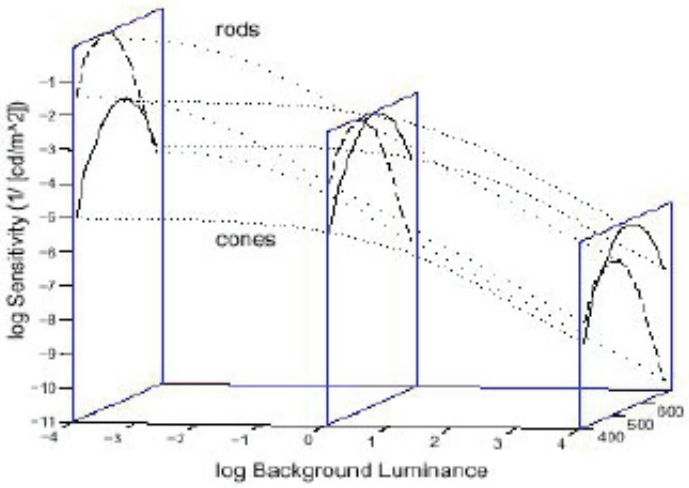

Figure 2.8 A model of threshold sensitivity as a function of wavelength and background luminance for the rods and cone systems, [14]

topic to photopic range. First, at low luminance levels vision will be achromatic since detection at all wavelengths is served by the rod system. As the luminance level is raised into the mesopic range, the cone system will become active and colors will begin to be seen beginning with the long wavelength reds and progressing toward the middle wavelength greens. Only at relatively high luminance will short wavelength blue targets begin to appear colored. [14]

We must differ between *light adaptation*, *dark adaptation* and *chromatic adaptation*. Dark and Light adaptations refer to the adjustment of the visual mechanism to changes in the rate at which radiant energy enters the eye. The chromatic adaptation refers primarily to the adjustment of the visual mechanism to changes in its spectral distribution [16].

Dark Adaptation

Dark adaptation is experienced as the temporary blindness that occurs when we go rapidly from photopic to scotopic levels of illumination. The slow time adaptation occurs for the dark adaptation means that vision can be impaired for several minutes when we move quickly from high illumination levels to low ones, [14]. The visual system is completely adapted after 35 minutes.

Light Adaptation

Light adaptation is the decrease in visual sensitivity upon increases in the overall level of illumination.When we go out quickly from low to high levels of illumination, at first everything is painfully glaring and we squint or close one eye to reduce the discomfort. However over time the overall brightness of the visual field diminishes to more comfortable levels and normal vision is restored [14]. The light adaptation of the rods system in the scotopic range is extremely rapid, it needs only 2 seconds. The cone system needs more time to adapt.

Chromatic Adaptation

Chromatic adaptation is the capability of the HVS to adjust to widely varying colors of illumination in order to approximately preserve the appearance of object colors [11].

2.5 Colorimetry

Colorimetry is the science of measuring colors. As stated before of this chapter (see 2 and 2.4), color depends on several factors as material properties, conditions of the observer, characteristics of the visual system and neural processes. Color could be seen as the result of the interpretation of the data, in the brain, collected by the visual system. The perception of color is defined as *color sensation*. The term color itself is used to identify a characteristic of the stimulus. The properties of color which are inherently distinguishable by the human eye are *hue*, *saturation* and *brightness*. The hue corresponds to the attributes of a color which let's us decide if it's "red", "blue", "green", "yellow", etc. Saturation is the colorfulness of an area judged in proportion to its brightness [11]. Pink may be thought of as having the same hue as red but being less saturated. A fully saturated color is one with no mixture of white. Brightness (or *lightness*) is the brightness of an area judged relative to the brightness of a similarly illuminated area that appears to be white or highly transmitting [11]. Pure white or black or grey are said *achromatic*. They do not have a *hue*. Colors that have hue are *chromatic*.

Spectral colors

The continuous range of spectral colors can be seen in a rainbow or by separating light with a prism. This corresponds to the visible spectrum. Spectral colors are composed of a single wavelength. The correlation between colors and wavelength can

be seen in figure 2.9.

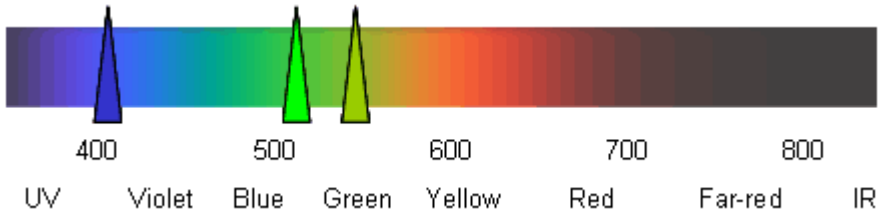

Figure 2.9 Spectral colors

Primary Colors

Any set of three colors which when added in appropriate combination will yield white can be considered to be primary colors. These 3 primary colors (**R**ed, **G**reen and **B**lue for example) can be used to map a color space. The coordinates of a point in space defines a color C by :

$$C = r\mathbf{R} + g\mathbf{G} + b\mathbf{B} \tag{2.7}$$

Where $\mathbf{R}, \mathbf{G}, \mathbf{B}$ are the unit vectors and r, g, b are the so called ***tristimulus values***.

2.5.1 Color Matching

The *Commission International de l'Eclairage* (*CIE*) is an institute in charge of defining the procedures and the standards for the use of color and colorimetry applications. In 1931 the CIE has defined a standard observer with a set of standard conditions for performing color measuring experiments. A big number of color matching experiments have been performed under these standardized conditions. In a color

matching experiment a person has to use 3 particular light sources, that emit light on a white screen where the 3 projections overlap and form an additive color mixture. On the other side of the screen a target color is projected which the observer tries to match by altering the intensities of the 3 light sources. Color matching studies showed that colored samples could be matched by combinations of monochromatic primary colors Red $700nm$, Green $546.1nm$ and Blue $435.8nm$. The results of a large group of observers could be reproduced by a set of the 3 color matching functions $\bar{r}(\lambda), \bar{g}(\lambda)$ and $\bar{b}(\lambda)$ shown in fig 2.10. As it is not possible to match all colors by additive mixture, some negative values are produced for the *red* color matching function. These negative values correspond to an addition to the target color instead of adding to the color obtained by mixing the 3 primaries. To get rid of the negative values, the CIE introduced their color matching functions $\bar{x}(\lambda), \bar{y}(\lambda)$ and $\bar{z}(\lambda)$. They use a new set of (imaginary) primaries, called X, Y, and Z which have the following properties:

1. They always produce positive tristimulus values
2. It is possible to represent any color in terms of these primaries
3. They where derived so that equal values of X, Y, and Z produce white
4. They were arranged so that a single parameter Y determines the luminance of the color
5. They are related to the sensitivity of the human eye by the use of color matching

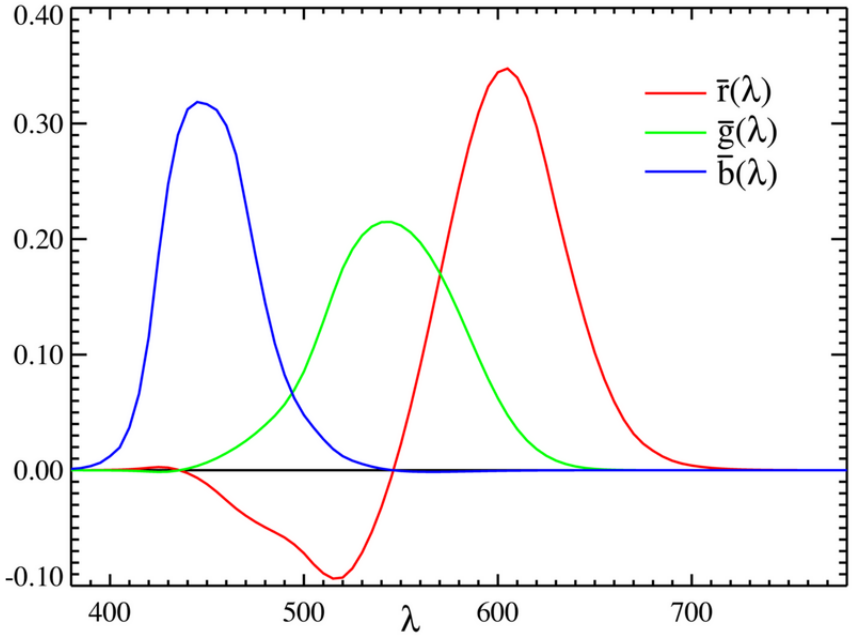

Figure 2.10 RGB Color Matching Functions, 1931

functions which match to the CIE 1931 Standard Observer.

2.5.2 CIE Chromaticity Diagram

As stated before (2.5.1 and see also Device Independent Color Spaces in section 2.5.3) the CIE Color Space is characterized by a luminance parameter Y and two color coordinates x and y. The coordinates x and y specify a point on the chromaticity diagram, see fig. 2.12. The spectral colors are distributed around the edge of the diagram. In theory any color can be expressed in terms of the two color coordinates x and y. The colors which can be matched by combining a given set of three primary colors (see 2.5) such as the red, green,and blue of a monitor or television screen, are represented on the chromaticity diagram by a triangle joining the coordinates for the

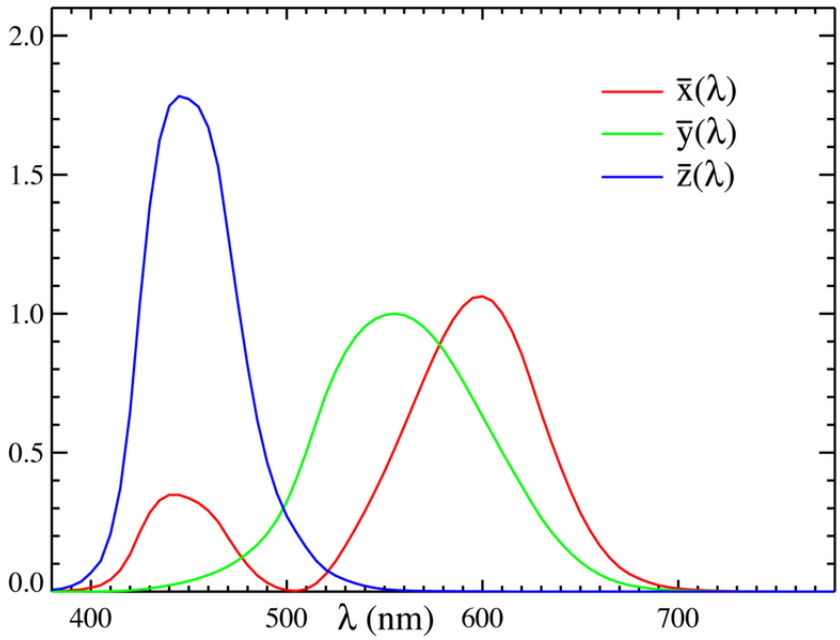

Figure 2.11 CIE XYZ Standard Observer Color Matching Functions

three colors. The Triangle represents the *color Gamut* of the monitor. So while the Gamut of normal human vision covers the entire CIE diagram, the Gamut of a RGB display device represents only a triangular region inside the CIE diagram.

2.5.3 Color Spaces

As mentioned before, three parameters are used to describe color information. Those three parameters define a ***color space***. For painting for example we can specify the amount of red color as the X axis, the amount of blue as the Y axis, and the amount of yellow as the Z axis, giving us a three-dimensional space, wherein every possible color has a unique position. Likewise for RGB. Another way of making the same colors is to use their hue (X axis), their saturation (Y axis) and their brightness

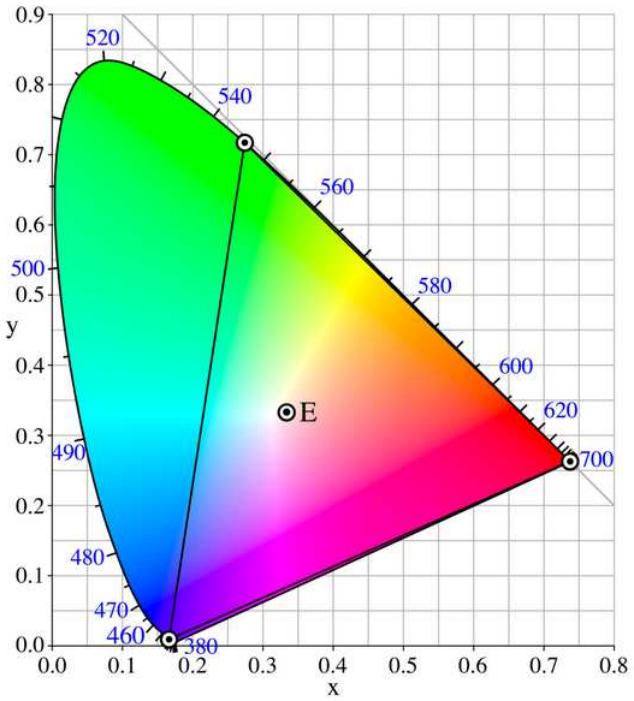

Figure 2.12 CIE Chromaticity Diagram

(Z axis). This is called the HSB or sometimes HSL (**H**ue **S**aturation **L**ightness) color space. In general we can differ between *device dependent* and *device independent* color spaces. In device dependent color spaces, the description of color information is related to the characteristics of a particular device (input or output). For example, in a monitor it depends on the set of primary phosphors, while in an ink-jet printer on the set of primary inks. This means that a color (e.g. R=250, G=20, B=150) will appear different when represented on different monitors. On the contrary a device independent color space is not dependent from the characteristics of a particular device. This means that a color represented in this color space always corresponds to

the same color information [1].

Device Dependent Color Spaces

RGB

The RGB (**R**ed **G**reen **B**lue) color space is the one used for monitors, scanners and digital cameras. The color space is a Cartesian Cube represented by the three primaries *Red*, *Green* and *Blue*.

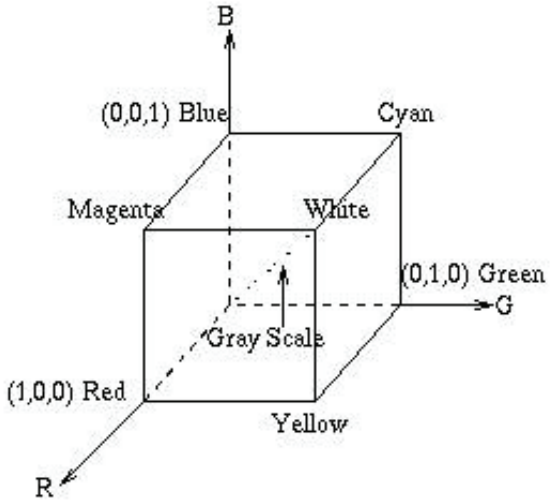

Figure 2.13 The RGB Cube

The RGB space is non uniform and not correlated with human perception, although it is an additive system (see fig. 2.14) and is based on the concept that the colors can be added to get a new one just like the human visual system mixes colors.

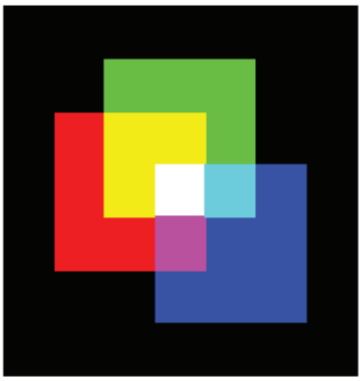

Figure 2.14 RGB, an additive color system

CMY

The CMY color space is, in contrast to the RGB color space, a subtractive color system. The colors are mixed by the selective removal of wavelengths from light which produces new colors. The structure of the color space is similar to the metric of the RGB color space. The subtractive primaries of the CMY color space are: *Cyan*, *Magenta* and *Yellow*. In the interval [0, 1], the color specification in the color space CMY can be obtained by its specification in RGB color space following the linear transformations:

$$C = 1 - R, M = 1 - G, Y = 1 - B \tag{2.8}$$

The formula 2.8 is a very simplified formula. This color space requires the full spectral knowledge of the CMY channels. This system is typically used with extra dark/black ink (CMYK) to obtain a higher contrast.

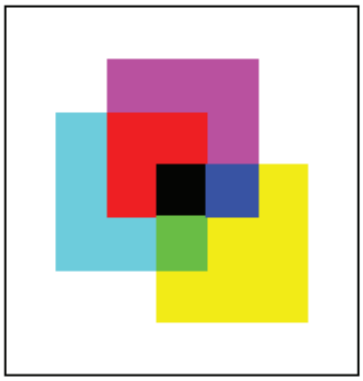

Figure 2.15 CMY, a subtractive color system

HSB

The HSB color space tries to represent color in a way more similar to human color perception. It breaks color into three components: *Hue*, which represents the "pure" color and is given by an angle in the range 0 to 360, the percentage of *Saturation* and the percentage of Brightness. This color space is useful for example for classifying colors.

sRGB

The ***standard RGB*** color space was created by Hewlett-Packard and Microsoft Corporation. It has been endorsed by the W3C, Exif, Intel, Pantone, Corel and many other industry players. It approximates the color gamut of the most common computer display devices and therefore tries to make a bridge between device dependent and device independent color spaces. The sRGB chromaticity coordinates can be seen in figure 2.16

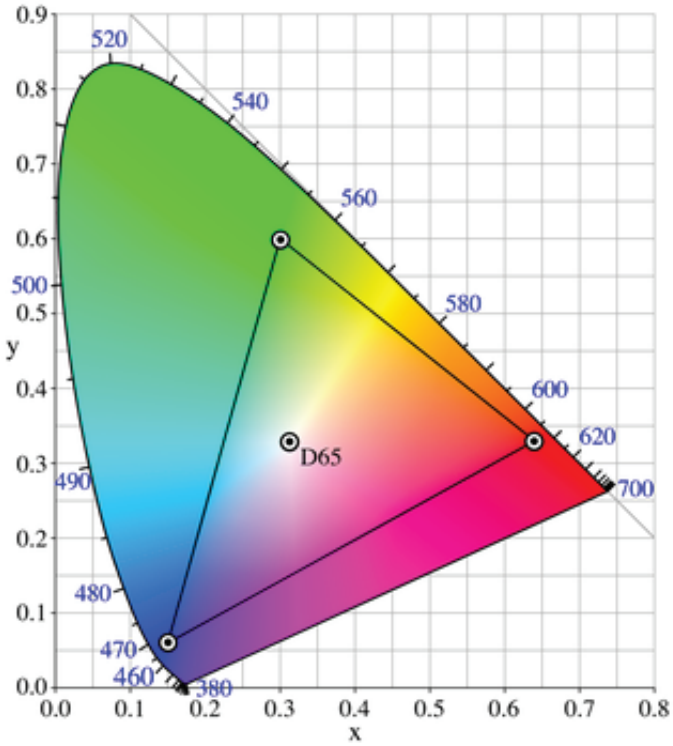

Figure 2.16 The sRGB color Gamut

Device Independent Color Spaces

The XYZ color space was defined by the CIE in 1931, in result of a series of experiments done in the late 1920's by W. David Wright and John Guild which led to the CIERGB color space from which the CIEXYZ color space has been derived. The idea was that all visible colors could be defined by using only positive values. The Y value represents the luminance. Just as the RGB color space the XYZ color space is non-linear. A color that is defined in this system is referred as Yxy, where Y is the brightness of the color and x and y are chromaticity parameters of the color which are functions of all three tristimulus values X, Y and Z:

$$x = \frac{X}{X + Y + Z} \tag{2.9}$$

$$y = \frac{X}{X + Y + Z} \tag{2.10}$$

A third coordinate, z can also be defined but is redundant since $x + y + z = 1$ for all colors. The X and Z tristimulus values can be calculated back from the chromaticity values x and y and the Y tristimulus value:

$$X = \frac{Y}{y}x \tag{2.11}$$

$$Z = \frac{Y}{y}(1 - x - y) \tag{2.12}$$

CIELab & CIELuv

The CIEXYZ color space is highly non-linear as can be seen in figure 2.17 which represents the MacAdam Ellipses. A MacAdam ellipse is the region on a chromaticity diagram which contains all colors which are indistinguishable, to the average human eye, from the color at the center of the ellipse.

In order to have linear color spaces for visual perception the CIE introduced the CIELab and CIELuv color spaces. The CIELab is based directly on the CIEXYZ. In CIELab coloring information is referred to the color of the white point of the system. The three parameters in the model represent the lightness of the color (L,

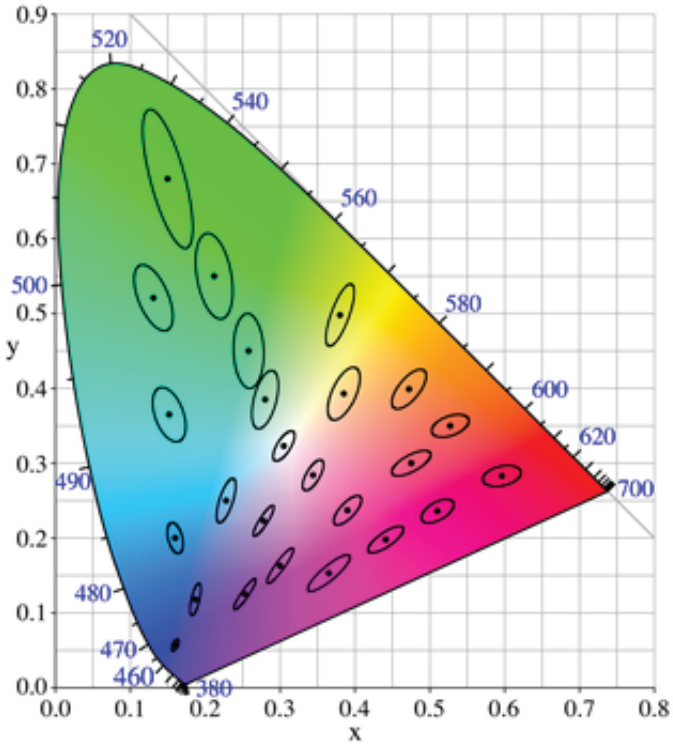

Figure 2.17 The MacAdam Ellipses on the CIE Chromaticity Diagram

L=0 yields black and L=100 indicates white), its position between magenta and green (a, negative values indicate green while positive values indicate red) and its position between yellow and blue (b, negative values indicate blue and positive values indicate yellow). CIELuv is also directly based on CIEXYZ and is another attempt to linearize the perceptibility of color differences. In CIELuv coloring also refers to the white point.

Chapter 3
Display Devices

As stated before (see 2.4.1), the human visual system is capable to produce accurate visual information in an impressive dynamic range. The goal of taking a digital picture or generating a CG scene is to display it properly on an output device. This might be an CRT monitor or a photographic print. There are 2 kinds of display medias: *light-emitting* (like CRT, LCD, Plasma Displays) and *light-propagating* (like photos, prints). Light-propagation displays do not emit their own light and therefor need an external light source. Unfortunately display devices have small dynamic range. The perfect display device should be able to reproduce an image as it would be seen by the human visual system. In other means it would have the possibilities to display luminance in the dynamic range of the HVS and should have the same color gamut. Since this is not yet possible we will give a little insight in the functionality of some display devices like CRT monitors, LCD monitors and Plasma devices. We will also talk about gamma correction.

3.1 CRT Monitors

CRT stands for *Cathode-Ray Tube*. A CRT Monitor consists of 7 basic components: *electron guns, control grids, accelerating plates, focusing structures, deflection structures, phosphor coating,* and *shadow mask*. See fig. 3.1

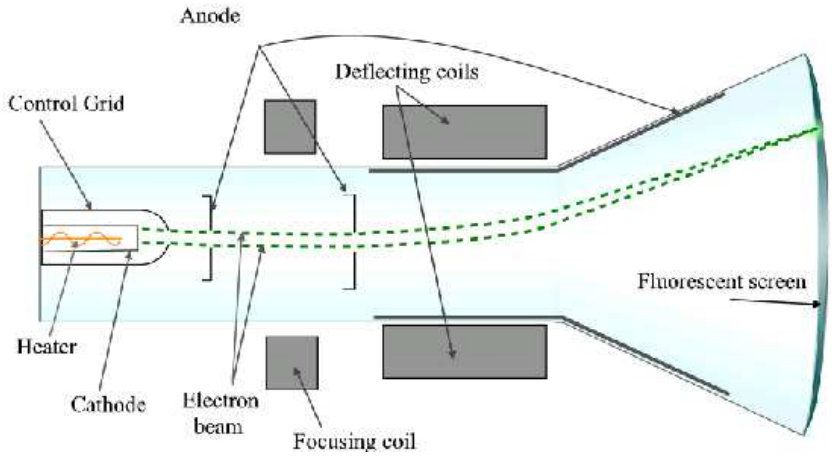

Figure 3.1 Cathode Ray Tube

A cathode produces electrons by heating and fires them at a controlled rate through the control grid. The accelerating plates increase the velocity of the electron beams, and the focusing structures act to sharpen the fuzzy beam of electrons [33]. The electron beam scans the monitor faceplate rapidly in a raster pattern (left to right, top to bottom), and the intensity of the beam is modulated during the scan so that the amount of light varies with the spatial position on the faceplate. The video voltage controlling the beam intensity is usually generated by a graphics card, which emits a new voltage on every tick of its pixel clock. The duration of each voltage sample determines the pixels width. Each pixel is a small fraction of a raster line painted on the phosphor as the beam sweeps from left to right [5]. Most CRT monitors are *multisync* which allows the characteristics of the raster to be determined by the graphics card. A color monitor contains 3 interleaved phosphore types: *red, green*

and *blue*. They are arranged in stripes (for monitors with aperture grille designs) or clusters (for monitors with shadow mask) across the monitor and each phosphore type has its own electron beam. Each beam can only reach one of the 3 specific colors. This is due to the mask or grille which absorbs electrons that would hit the wrong phosphor. The illustration fig. 3.2 shows:

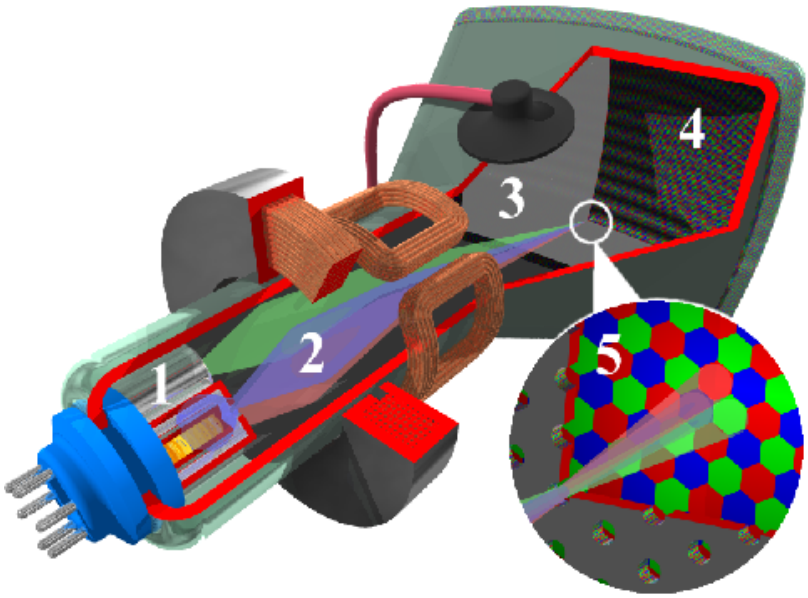

Figure 3.2 Cathode Ray Tube interior

1. Electron guns

2. Electron beams

3. Mask for separating beams for red, green and blue part of the displayed image

4. Phosphor layer withe red, green and blue zones

5. Close-up of the phosphore-coated inner side of the screen

Each pixels light could be interpreted as the combination of the light emitted red, green and blue phosphores. Let $C(\lambda)$ be the light emitted from a single pixel, then,

$$C(\lambda) = rR(\lambda) + gG(\lambda) + bB(\lambda) + A(\lambda), \tag{3.1}$$

where λ represents wavelength, $R(\lambda)$, $G(\lambda)$, and $B(\lambda)$ are the spectra of light emitted by each of the monitors phosphors when they are maximally excited by the electron beam, r, g, and b are real numbers in the range $[0, 1]$, and $A(\lambda)$ is the ambient light emitted (or reflected) by the monitor when the video voltage input to the monitor is zero for each phosphor. The values r, g, and b are referred as the phosphor light intensities.

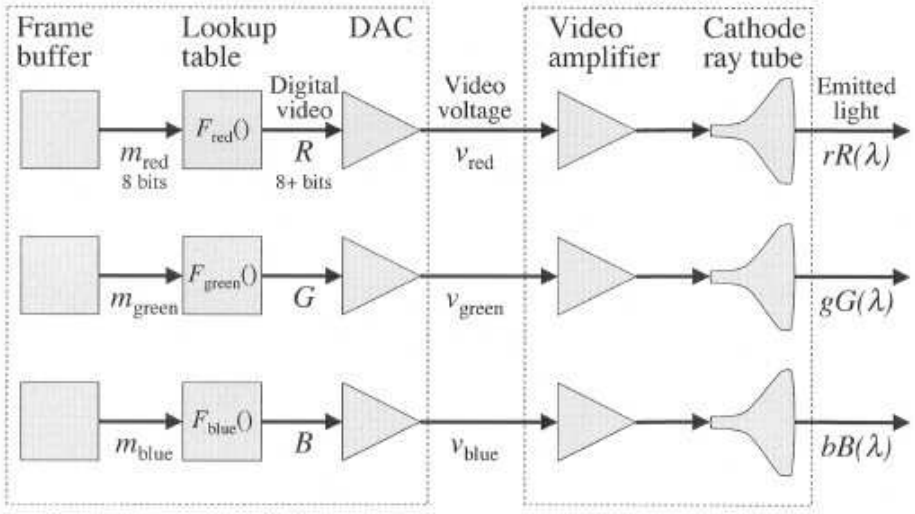

Figure 3.3 Pixel processing, [5]

Figure 3.3 shows how a pixel is processed. The graphics card generates the video voltage based on the digital values stored in the on-board memory. These digital values can be written into two components of graphics card memory: frame buffer and lookup table [5].

3.2 LCD Panels

LCD monitors are the dominant technology for laptop computers but they are also more and more common for desktop computers. They were designed as a flat equivalent of the CRT monitors. LCD stands for *Liquid Crystal Display.* The most common LCDs for computers are backlit AMLCDs of the *twisted nematic* type. Twisted Nematic displays contain liquid crystal elements which twist and untwist at varying degrees to allow light to pass through. When no voltage is applied to a TN liquid crystal cell, the light is polarized to pass through the cell. In proportion to the voltage applied, the LC cells twist up to 90 degrees changing the polarization and blocking the lights path. By properly adjusting the level of the voltage almost any grey level or transmission can be achieved. These LCDs are manufactured by deposition and patterning of (active) pixel electronics on a glass substrate. Color displays are produced by laying a mosaic of red, green, and blue colored filters on the substrate glass aligned with the pixel array [28]. Usually the individual RGB pixels are rectangular and arranged so that threes horizontally adjacent rectangular RGB pixels constitute a single square color pixel. Thus the display appears to be composed of stripes of

rectangular RGB pixels going vertically across the screen. The backlight is typically a fluorescent lamp with three prominent peaks in the red, green, and blue regions of the spectrum. In most AMLCD color monitors, the RGB pixels are driven and controlled independently. The emitted light is combined and averaged in the eye, just as in the CRT monitor [28].

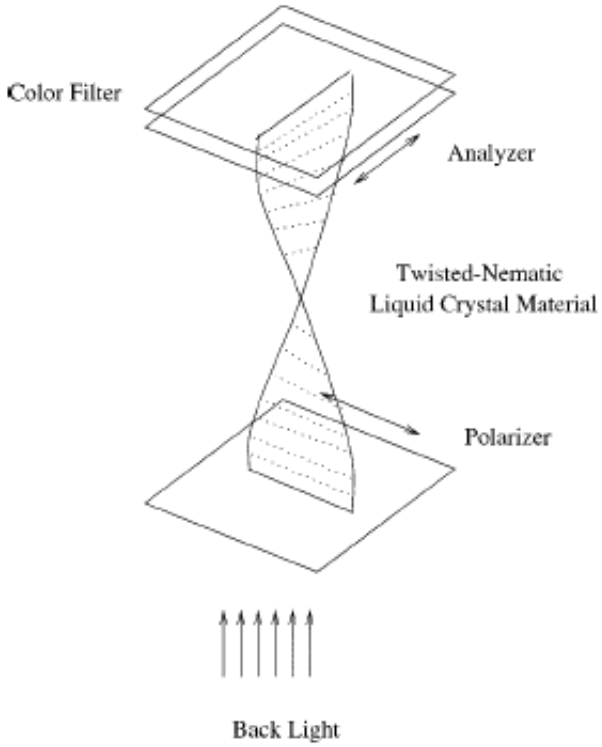

Figure 3.4 Structure of LCD pixel, [28]

A drawback of LCDs is the *angular dependence*: The optical filtering properties of LCD panels can have a strong angular dependence, so it is important to consider the observers viewing position when characterizing LCD displays. This is especially important if the observer will be off-axis or there will be multiple observers. Angular

dependence may be the greatest obstacle to the use of LCDs for accurate rendering [5].

3.3 Plasma Displays

Plasma displays are based on the emission of gas radiation. When gas is ionized it emits radiations. High voltage is applied to the gas by bathing a pair of electrons within the gas. A matrix of intersecting rows and columns of electrodes is used as display [33]. Plasma displays are much more expensive than CRTs and LCDs but are currently favored by museums for example, because the plasma display is both flat like an LCD and nearly lambertian: emitted light is independent of the viewing angle like a CRT.

3.4 Gamma Correction

Gamma correction is an internal adjustment for rendering in photography, television and computer imaging. The gamma symbol γ represents a numerical parameter that describes the nonlinear relationship between pixel value and luminance. It is preferable for reasons of perceptual uniformity to establish a non-linear relationship between color values and intensity or luminance. A conventional CRT has a power-law, called the *gamma-law*, which corresponds a non-linear relationship between voltage and intensity.

$$I_{out} = K \cdot v^{\gamma} \tag{3.2}$$

The output intensity I_{out} is equal to some constant,K, times the input voltage v raised to a constant power γ. Usually CRT monitors follow a power relation corresponding to a 2.5 γ value. The sRGB standard intentionally deviates from this value to something a target γ of 2.2, such that images get a slight contrast boost when displayed on a conventional CRT even though most CRT monitors do not have a γ 2.2 [29]. The functions associated with the three guns of a color CRT monitor are not

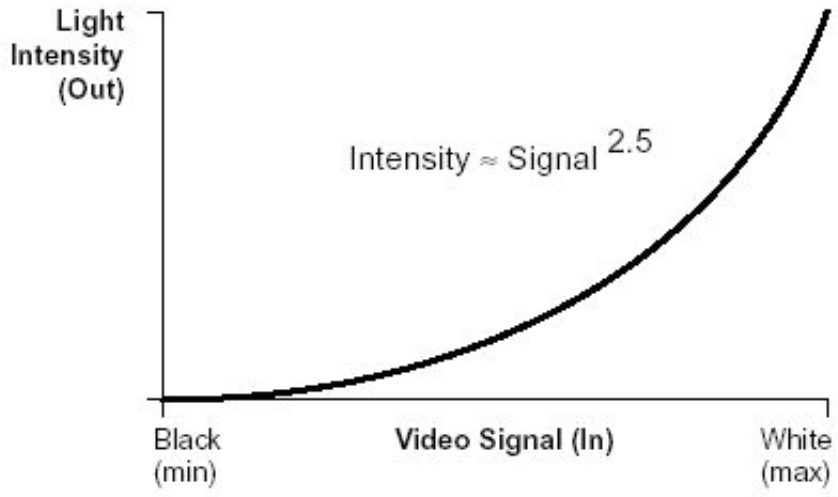

Figure 3.5 Power function with gamma 2.5 of a CRT

necessary identical. The process used to correct this non-linearity, in order to achieve correct reproduction of the intensity, is called *gamma-correction* [24]. In the context of color science, the gamma-correction process defines the right gamma value for the

three guns of the CRT monitor and the parameters of the function that describes this non-linearity. This function is also called electro-optical transfer function (TF). The TF describes the relationship between the signal used to drive a given monitor channel and the luminance produced by that channel. In the case of a LCD monitor the TF has a different shape than the TF of a CRT monitor. Fairchild and Wyble

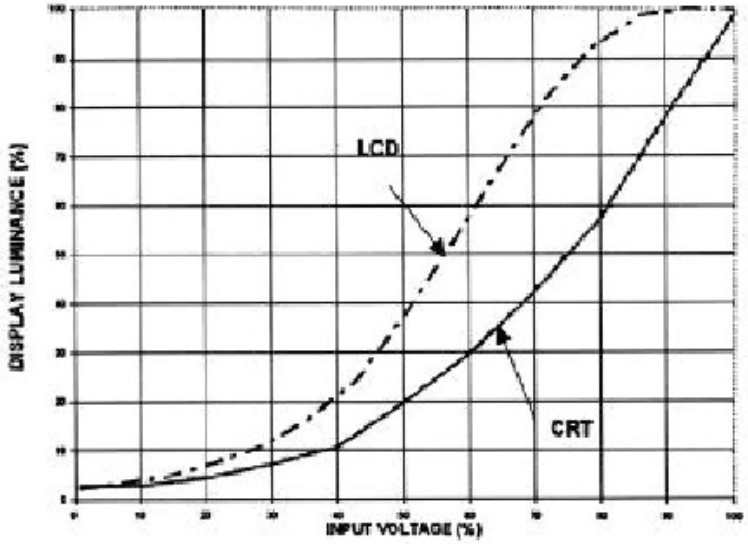

Figure 3.6 TF's of a LCD monitor and a CRT monitor, [12]

[12] showed that while the raw physical performance of a LCD differs from that of a CRT, the digital drive circuitry for a general-purpose LCD monitor would be designed to mimic a CRT behavior. Thus, the images presented to an user appear similar to those expected from a CRT monitor driven by a computer video output. In this way the TF of a LCD mimics the typical TF of a CRT display [1].

Chapter 4
Tone Mapping Methods

Compressing the range of values of an image for the purpose of display on a low dynamic range display device is called ***tone mapping*** or ***tone reproduction*** [29]. According to [39] there are two important criteria's for a reliable tone mapping: reproduce the *visibility* and the *subject experience* of the real world observer. The visibility is reproduced when we see the same scene details, which we see in the real scene. In other words, there are not objects obscured in the under-or over-exposed regions in the digital image, and the features are not lost in the middle. Reproducing the subject experiences of the real world observer means reproducing the overall impression of the brightness, contrast, and color [1]. Nevertheless the goal of tone mapping is not to enhance the image by showing more information then one would see in real life but to *simulate* the visibility and the contrast (not to maximize it). We must differ between global and local approaches. Global methods use the same function for each image pixel and local methods modulate compressive functions by pixel neighborhood. We will not try to directly compare the different methods since the decision of quality and performance are varying between individuals. First in 4.1 an overview of global operators is given and then in 4.2 an overview of some local methods will be discussed.

4.1 Global Operators

Tumblin and Rushmeier [34] gave name to Tone Mapping in 1993. They proposed a tone mapping operator which should preserve the viewer's overall impression of brightness. The operator is based on the super-threshold brightness measurements made by Stevens and Stevens [32] according to whom a power-law relation exists between luminance L (the quantity of light in the visible range), and perceived brightness B (the subjective impression of the viewer).

$$B = k(L - L_0)^{\alpha} \tag{4.1}$$

where k is a constant, L_0 is the minimum luminance that can be seen and α is an exponent between 0.333 and 0.49. This model is not valid in complex scenes but was chosen by Tumblin and Rushmeier do its low computational costs. To preserve the overall impression of brightness in the scene they used one adaptation value for the real scene and another adaptation value for the displayed image. Because a single adaptation level is used for the scene, though, preservation of brightness in this case is at the expense of visibility. Areas that are very bright or dim are clipped, and objects in these areas are obscured. [39]. Further in 1999 Tumblim claims that this first method has some major drawbacks: first, scenes that approach total darkness are displayed as anomalous middle grey images instead of black. Second, the display contrast for very bright images is unrealistically exaggerated. Also this operator did not address the contrast limitation of displays and was presented in an awkward form

that discouraged its use [35].

As for the global operators one must in general differ between 3 main approaches:

- Linear Scaling
- Logarithmic scaling
- Histogram-based compression

4.1.1 Linear Scale-Factor Methods

Although the human visual system certainly does not use a linear scaling function to adapt to different dynamic ranges, these methods can perform acceptable for a wide range of pictures. And being simple to implement and fast to use, most of the modern digital photo cameras use a simple linear scaling method. As long as the dynamical range is not too high, results can be satisfying.

The idea behind Linear Scale-Factor Methods is to map the maximum radiance L_{max} to 1,

$$n = \frac{L}{L_{max}} \tag{4.2}$$

As stated in [18] this mapping is useless if the light source is visible or the image contrast is too high. In that final case the result-image will be too dark.

Mean Value Mapping

The most common application of linear Scale-Factor Methods is the Mean Value Mapping. In fact this method is implemented in most digital cameras. The idea is to map the average radiance L_{ave} to 0.5, hence the new maximum value $2 \times L_{ave}$ to 1 and clip everything beyond the new maximum value to 1.

$$n = 0.5 \cdot \frac{L}{L_{ave}} \tag{4.3}$$

The information in the range $[2 \times L_{ave}, L_{max}]$ will be lost. This might be catastrophic for some images. Especially when the image histogram of the picture is Bi-modal. The average value would lie somewhere between the 2 main parts of the histogram and the maximum value might miss the second main part of the histogram and discard extremely valuable information. Also if used on pictures with a very high or very low average reflectance the results will be unsatisfying. For example a picture of a snowy mountain would get too dark by mapping the average to 0.5. Another problem is the case when few very high radiance values increase the average too much, making the final image too dark. As one can see the method has some major drawbacks but the simple implementation and the fast computation of this method are the reason of the wide use of it in digital photography.

Ward's Contrast Based Scale-Factor

The idea behind Ward's method [37] was to display bright scenes as bright and poorly lit scenes as dark on a display. Hence, this method should preserve the visibility of the original scene. Ward wanted to find a proportionality constant between display luminance and world luminance that yields a display with roughly the same contrast visibility as the actual scene. Therefore he proposed a light-dependent multiplying factor m to restore the appearance of different lighting conditions. The factor m was deduced using the experimental data obtained by Blackwell [4] who established -under precise laboratory conditions, which differ from complex natural viewing conditions- the following relationship between the adaptation luminance L_a and the minimum discernible difference in luminance:

$$\Delta L(L_a) = 0.0594 \cdot (1.219 + L_a^{0.4})^{2.5} \tag{4.4}$$

Blackwell showed that the smallest noticeable increase in luminance or "contrast threshold" of a small target on a uniform background grows non linearly as the amount of surrounding light increases. Using Blackwell's results, Ward wanted to find m such that:

$$L_d = m \cdot L_w \tag{4.5}$$

Where L_d is the display luminance at an image point and L_w is the original scene or world luminance. Both are measured in cd/m^2.

To get the value m he assumed that

$$\Delta L(L_{da}) = m \cdot \Delta L(L_{wa}) \tag{4.6}$$

with $\Delta L(L_{da})$ being the minimum discernible luminance change at L_{da}, L_{da} is the display adaptation luminance and L_{wa} is the world adaptation luminance. With this assumption one can solve equation 2.11 using the property from equation 2.9 and get for m:

$$m = \left[\frac{1.219 + L_{da}^{0.4}}{1.219 + L_{wa}^{0.4}}\right]^{2.5} \tag{4.7}$$

This simple linear scale-factor yields good results for a wide range of applications where lighting simulation is important as architecture visualization for example.

4.1.2 Logarithmic Compression

Logarithmic compression is a non-linear functional shape which is used to reduce the dynamic range of an image:

$$L_d(x, y) = \frac{log(1 + L_w(x, y))}{log(1 + L_{w,max})} \tag{4.8}$$

The base of the logarithm is not specific in the above equation and can be freely chosen.

Drago et al. Logarithmic Mapping

In 2003 Drago et al. [9] introduced a Tone Mapping Operator based on logarithmic compression of luminance values, imitating the human response to light. As

stated before the base of the logarithm can be freely chosen. Drago et al. made the base of the logarithm as a function depending on each pixel's radiance. Luminance values from $log_2(L_w)$ to $log_{10}(L_w)$ are interpolated to provide good contrast and detail preservation in dark areas while compressing high luminance values. The arbitrary choice of the base is done by using the basic property of logarithm :

$$log_{base}(x) = \frac{log(x)}{log(base)} \tag{4.9}$$

The computed value for each displayed pixel L_d is given by:

$$L_d = \frac{L_{dmax} \cdot 0.01}{log_{10}(L_{wmax} + 1)} \cdot \frac{log(L_w + 1)}{log\left(2 + \left(\left(\frac{L_w}{L_{wmax}}\right)^{\frac{log(b)}{log(0.5)}}\right) \cdot 8\right)} \tag{4.10}$$

Where L_w is the luminance pixel of the scene, L_{wmax} is the maximum luminance of the scene and both values are normalized by L_{wa} (luminance world adaptation) and scaled by an exposure factor. L_{dmax} is the maximum luminance capability of the display medium.

4.1.3 Histogram-Based Compression

Ward et al. 1997

Ward et al. [39] presented a tone mapping operator based on iterative histogram adjustment and spatial filtering. This operator ensures that contrasts that exceed human visibility thresholds in the scene remain visible on the display while reducing high scene contrasts. Any form of halo artefact or local gradient reversals are avoided.

Various aspects of the HVS are also taken into account: glare, color sensitivity and visual acuity. The way to obtain the glare effect is based on the computation of a low-resolution veil image from foveal sample values. They then interpolated this veil image by adding glare effect to the original image. In their method they take a histogram of scene brightness which correspond with foveal adaptation levels for possible points in an image. They obtain a histogram and a cumulative distribution function. Ferwerda et al's threshold sensitivity data is then used to compress the original dynamic range to that of the display device [7]. This global method uses some local filtering for the simulation of visual effects.

4.2 Local Operators

Here some local methods will be discussed but since this work is about a new global method, we will not discuss every method out there but some of the most important ones. Some examples can be seen in the Results chapter 6.

4.2.1 Chiu et al. 1993

Chiu et al. [6] where the first to try a non-global approach to tone mapping. Because of the HVS being more sensitive to relative then to absolute changes in luminance they developed a spatially non-uniform scaling function for high contrast images. They argument that slow spatial variation in luminance may not be very perceptible by the HVS because the eye is more sensitive to reflectance than luminance.

Translated to images with higher dynamic range then the display device this means that they can be displayed without much noticeable difference if the scaling function has a low magnitude gradient. By blurring the image to remove high frequencies, and inverting the result, the original details can be reproduced, but reverse intensity gradients appear when very bright and very dark areas are in close proximity [7]. Their work is based purely on experimental results and therefore not as robust as other operators. Being a local method it has high computational costs.

4.2.2 Fattal et al. Gradient Domain Model

Fattal et al. [13] presented in 2002 a Tone Mapping method which is computationally efficient and robust. The idea relies on the assumption that the HVS is not very sensitive to absolute luminance reaching the retina, but rather responds to the changes of local intensity ratio. They observed that any drastic change in the luminance across a high dynamic range image must give a rise to large magnitude luminance gradients at some scale whereas fine detail corresponds to gradient of much smaller magnitude. They manipulate the gradient field of the luminance image by attenuating the magnitudes of large gradients. A new, low dynamic range image is then obtained by solving a Poisson equation on the modified gradient field. They offer an effective and easy-to-use tone mapping method which doesn't account for perceptual accuracy.

4.2.3 Reinhard et al. Photographic Approach

In 2002 Reinhard et al. [25] proposed a tone mapping method based on a photographic method known as *Zone System* defined by Ansel Adams in 1980. The Zone System approach divides a scene into 11 print zones ranging from pure black (zone 0) to white (zone X). Zone V represents a subjectively-defined middle-grey tone. Luminance readings are taken for light and dark regions and a dynamic range can be determined. An appropriate choice for the middle-grey ensures that the maximum possible detail is retained. A scaling similar to setting photographic exposure is applied, then highlighting and darkening selected regions (known as "dodging and burning" in photography) allows contrast to be controlled locally in the image over regions bounded by high contrast [7]. The method works well over a wide variety of HDR images. But it is limited to photographic dynamic range rather than the wider computer graphics dynamic range, and it also comes with high computational costs.

4.2.4 Visual Effects in Tone Mapping

In 2005 Krawczyk, Myszkowski and Seidel [17] presented a tone mapping operator which deals with perceptual effects of the HVS. Since adaptive methods which try to imitate the HVS often create an excess of details which sometimes take the credibility or the realism of the scene. The method described in [17] takes glares and visual acuity into account, as seen in fig. 4.1 in the top right image a computer generated scene is

visible with a glare effect for realism which would appear in the real-world perception while the left version is a local tone mapped version without perceptual effects. The bottom images are a daylight and a night scene of one picture. The close-up shows the area around the car in such way that their brightness match to illustrate the loss of visual acuity and the scotopic vision.

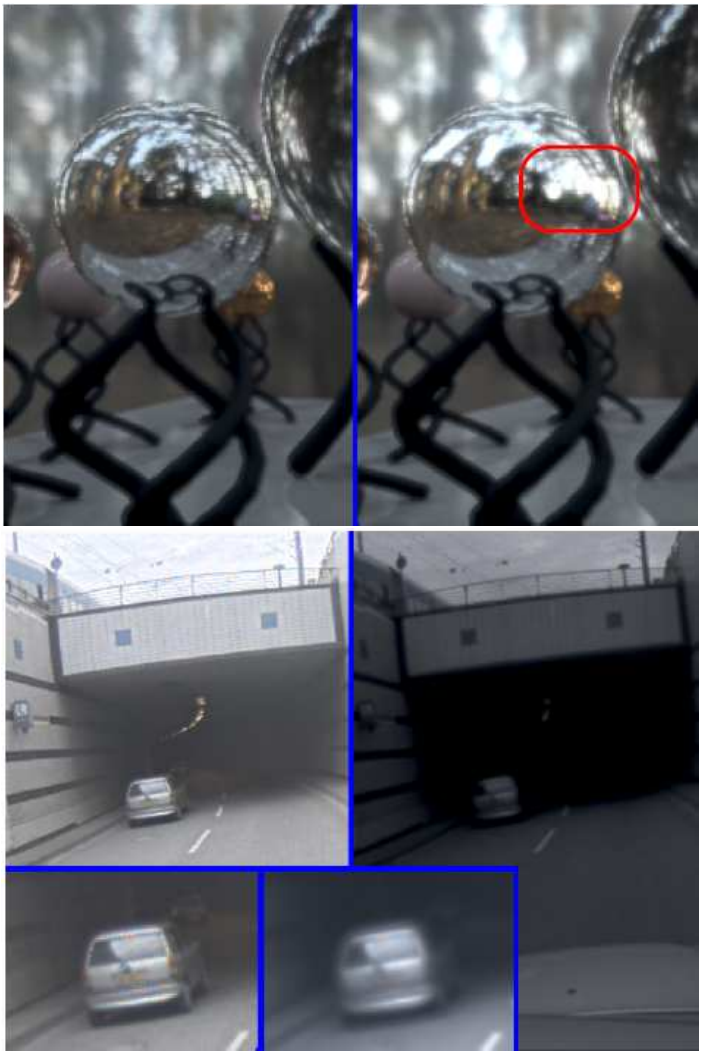

Figure 4.1 Perceptual Effects in Tone Mapping

4.3 Summary

The table in figure 4.2 taken from [7] shows a summary of most of the tone mapping methods and also gives some attributes of them. It holds most of the global methods [34], [37], [14], [38], [35], [23], [26], and [10](in the table referred to as *Spatially Uniform*), the local methods [6], [30], [15], [22], [36], [3], [13] and [25] (in the table referred to as *Spatially Varying*) and some methods ([14], [23] and [10]) which do account for temporal differences (like adaptation over time for exemple) which they refer to as *Time Dependent*.

Algorithm	Spatially Uniform	Spatially Varying	Time dependent	Strengths and Weaknesses
Tumblin and Rushmeier 1993	✓			Preserves brightness. Does not preserve visibility or account for adaptation. Grey scale only.
Chiu et al 1993		✓		Preserves local contrast. Ad hoc. Computationally demanding. Halo artifacts.
Ward 1994	✓			Preserves contrast - crucial for predictive lighting analysis. Clipping of very high and very low values. Does not consider complexities of typical workplace viewing.
Schlick 1994		✓		Speed and simplification of uniform and varying operators. Ad hoc - no perceptual accuracy.
Spencer et al. 1995		✓		Greater dynamic range through glare effects.
Ferwerda et al. 1996	✓		✓	Accounts for changes in threshold visibility, colour appearance, visual acuity and sensitivity over time. Psychophysical model. Useful for immersive displays.
Ward Larson et al. 1997	✓			Histogram equalisation. Preserves local contrast visibility. Uses models for glare, colour sensitivity and visual acuity to increase perceptual realism.
Jobson et al. 1997		✓		Multi-scale retinex model - perceptually valid. Problems with monochrome scenes and maximum contrasts outside 24-bit RGB range.
Pattanaik et al. 1998		✓		Multi-scale psychophysical representation of pattern, luminance and colour processing resulting in increased perceptual fidelity. Does not incorporate temporal aspects.
Tumblin et al. 1999	✓			Layering method for static, synthetic images. Foveal method for interactive scenes.
Tumblin and Turk 1999		✓		LCIS method preserves subtle detail and avoids halo artifacts.
Pattanaik et al. 2000	✓		✓	Psychophysical operator with time-dependent adaptation and appearance models. Does not support local adaptation.
Scheel et al. 2000	✓			Interactive method using texturing hardware. Does not account for adaptation over time.
Durand and Dorsey 2000	✓		✓	Interactive method with time-dependent adaptation and simulation of visual acuity and chromatic adaptation.
Ashikhmin 2002		✓		Preserves image details and absolute brightness information. Uses simple functional perceptual model. Simple to implement with moderate computational efficiency.
Fattal et al. 2002		✓		Computationally efficient and simple operator. Does not attempt psychophysical accuracy.
Reinhard et al. 2002		✓		Method based on photographic technique. Suits a wide variety of images, but limited to photographic dynamic range rather than the wider computer graphics dynamic range.

Figure 4.2 Summary and attributes of most Tone Mapping methods, [7]

Chapter 5
Extended Minimal Information Loss Methods

In this chapter the new minimal information loss methods created for this work will be discussed. The minimal information loss method was used for tone mapping by Neumann, Matkovic and Purgathofer in 1998 in their work [20]. It is a global tone mapping operator which tries to follow, in a certain way, a photographer's approach. Exposure is determined automatically by selecting the ideal clipping interval so that a minimum of information is lost, hence to obtain a minimum of detail-less image parts. It preserves the contrast of all correctly displayed pixels. This new methods, just as the original one, don't try to simulate perfectly the human visual system as the method [17] presented in 4.2. The methods presented here show an intuitive real time approach with better results then most of the local approaches.

5.1 Clipping Interval

The main goal of this method is to find the optimal clipping interval $[A, B]$ such that $B = C \cdot A$ where C is the given clipping contrast.

5.1.1 Photographic Approach

In non-professional photography the mean light intensity method is the most common method used (see 4.1.1). According to Morvay [19] the method gave good results in 80% of amateur motifs. In the remaining 20% the aperture has to be shifted to

obtain an optimal result. Furthermore this result only includes standard motifs. If the image histogram is bimodal results can be very unsatisfactory with this method. For example if the main subject is in shadow, an average measure causes the main subject to appear only as a silhouette. To get all the desired details the aperture has to be opened by 2 or 3 units, compared to the measured mean value.

5.1.2 Optimal Clipping Interval

As stated before, we are looking for the interval $[A, B]$ such that $B = C \cdot A$. The clipping contrast C depends on the display media, and should equal the maximum displayable medium contrast [20]. The clipping is done by setting all values smaller then A to A and all values bigger then B to B, with a minimum of information lost. In former approaches each color component was considered as equally important. In [20] they also discuss an approach where the pixel is considered to be the essential information unit, so the number of affected pixels would be minimized. They call this approach *minimum area loss*. In this work the use of the $max(r, g, b)$ function is introduced. This function can be combined with the original minimum information loss method. We also introduce the minimum information loss method with an new error function which leads to impressive results combined with the $max(r, g, b)$ function.

5.2 Log2 Image Histogram

The optimization process is done on a logarithmic image histogram. The histogram is built exactly as in the previous version of this method. The log_2 base is used in analogy to photography (every other base would work just fine as well). Since this function is not defined for 0, first all values that are smaller than a certain minimum value L_{min} ($log_2(L_{min}) = l_{min}$) should be set to this minimum value and, as the size of the histogram array is limited, the values above a certain maximum value L_{max} ($log_2(L_{max}) = l_{max}$) should be set to this value. Each array member of the histogram holds the number of pixels with the corresponding luminance. The luminance values for each pixel in the raw image are stored in float format, so actually each histogram array member represents luminance in a certain interval. The intervals of the histogram are equidistant and arbitrarily long, but a finer histogram yields a more precise result [20].

We define the histogram array as $H[k]$, where $k \in [1, k_{max}]$, the value l_{min} corresponds to $H[1]$ and l_{max} to $H[k_{max}]$. The luminance corresponding to $H[k]$ will be called L_k hence $log_2(L_k) = l_k$. The elementary histogram interval is δ defined as:

$$\delta = \frac{l_2 - l_1}{k_{max}} \tag{5.1}$$

The size of the clipping interval for a given clipping contrast C is called CLIP and defined as

$$CLIP = int(log_2(C)/\delta) \tag{5.2}$$

A possible choice for the values could be: $L_{min} = 2^{-20}$, $l_{min} = -20$, $l_{max} = 20$, $C = 45$ and hence $CLIP$ would be 1098. In this case histogram interval $\delta = 0.005$ which corresponds approximately the interval the human visual system is able to distinguish. The histogram array is initialized to zero and then $H[k]$ is incremented with

$$k = int\left(\frac{log_2(d) - l_{min}}{\delta}\right) \tag{5.3}$$

where d stands either for each color component r, g, or b (there would be three times as much entries in the histogram as pixels in the raw image) or the histogram can be filled with the $max(r, g, b)$ values (the histogram would then hold exactly as much entries as the raw image has pixels). Of course one could also fill the histogram with the values of all 3 color channels plus the $max(r, g, b)$ values or add the $max(r, g, b)$ more often.

5.3 Principle Of The Max(r,g,b)

The $max(r, g, b)$ function takes only the value of the color component with the highest value of the rgb triplet. The result is one value per color channel. The idea was proposed by Attila Neumann for Incident Light Metering and was described in [21]. In incident light metering the intention is to find a scalar value f that represents the irradiance value with the aim to reproduce the originally selected colors as faithfully as possible. For a given rgb triplet this value f can be : $f(r, g, b) = Y(r)+Y(g)+Y(b)$, where Y represents the CIE Y value which corresponds to the relative lightness and

has a maximum value of 100 [21]. Full red would have a lightness of 20, full green a lightness of 70 and full blue only a lightness of 10.

f can also be presented by the $max(r, g, b)$ function: $f(r, g, b) = max(r, g, b)$.

Let's consider an example: take a sample scene that consists of a homogeneously lit square, which lies normal to the viewing direction. One quarter of this square is *medium red*: $Y(r) = 0.5 * 20 = 10$ and $(r, g, b) = (0.5, 0, 0)$. The second quarter is *medium green*: $Y(g) = 0.5 * 70 = 35$ and $(r, g, b) = (0, 0.5, 0)$. The third quarter is *medium blue*: $Y(b) = 0.5 * 10 = 5$ and $(r, g, b) = (0, 0, 0.5)$ and the last quarter is neutral, *medium gray*: $Y(n) = 0.5 * 100 = 50$ and $(r, g, b) = (0.5, 0.5, 0.5)$. If this scene is lighten with an homogeneous neutral light $(r, g, b) = (1, 1, 1)$ the irradiance metering would yield a neutral color which should be scaled with $Y = 100$ or $(r, g, b) = (1, 1, 1)$. The resulting colors will be the same as in the original scene: medium red, medium green, medium blue and medium gray.

If we would lighten the scene with a blue light $(r, g, b) = (0, 0, 1)$ the light metering would measure a lightness of $Y = 10$ which would lead us to use a scaling factor of $100/10 = 10$, which will cause for an highly overexposed result (10 times overexposed) for all visible colors: the red and green square would be black (as they have no blue component), the blue square would be displayed as $(r, g, b) = (0, 0, 1)$ (after clipping) instead of the original $(r, g, b) = (0, 0, 0.5)$ as well as the medium gray quarter.

The same is to expect using red light, while the blue and green quarter would be displayed as black, the red and gray square would be highly overexposed. Also with green lighting the overexposure occurs. The irradiance of the scene lighten by green light $(r, g, b) = (0, 1, 0)$ would be $Y = 70$ and the scale factor $100/70 = 1.42$. The green and gray square would be displayed with the values $(r, g, b) = (0, 71, 0)$.

By using the $max(r, g, b)$ method which computes the irradiance value for each diffusor and stores only the maximum value the results of the experience above would be as follows:

With white, red, green, and blue lighting the new (fictive) irradiance value would be 1 and the scale factor would also be 1. For white lighting the result would be the same as before. Using blue lighting, the red and green square would be black. The medium blue and medium gray would be correctly displayed as medium blue $(r, g, b) = (0, 0, 0.5)$

The maximum method would also yield correct results for red and green lighting. This method always gives correct or at least better results then the Original Y method. For neutral lighting the max(r,g,b) method gives the same result, for unsaturated lighting it gives a similar result and for saturated lighting it gives significantly better results than the "Y approach" widely used in photography [21].

5.4 Search for the Clipping Interval

5.4.1 Original Algorithm

```
error :=0;
for i := CLIP + 1 to kmax do
    error += H[i];
leasterror := error;
best := 1;
for j := 1 to kmax - CLIP do
    begin
       error +=H[j];
       error -= H[j + CLIP];
       if error <= leasterror then
           begin
              leasterror :=error;
              best := j + 1
           end
    end
```

Figure 5.1 Original Algorithm [20]

The original version applies a discrete algorithm on the log_2 histogram. The length of the clipping interval is CLIP and the optimal position is found by shifting the interval along the complete histogram in discrete steps of one, looking for the position where the information outside the clipping interval is minimal. The error function used in the original version is therefor a simple $0-1$ type discrete error function (see fig. 5.2).

The pseudo code of this algorithm is given by fig. 5.1.

Figure 5.2 Simple Error Function

In each step the error sum is increased by the outgoing histogram member and decreased by the incoming one. The calculated optimal clipping then starts at `H[best]`, and ends at `H[best+CLIP-1]`. The algorithm runs in linear time $O(k_{max})$.

The actual interval $[a, b]$ on the logarithmic scale is then:

$$a = l_{min} + best \cdot \delta \tag{5.4}$$

$$b = a + c \tag{5.5}$$

hence on the linear scale:

$$A = 2^a \tag{5.6}$$

$$B = A \cdot C \tag{5.7}$$

Now the clipping can be done at $[A, B]$ and the result image can be generated.

5.4.2 New Error Function

The algorithm presented in 5.4 treats every pixel outside of the clipping interval alike. Since it's a 0-1 discrete error function it does not matter if the pixel outside the clipping interval is very close to B or far away from it. Therefor we can consider

other types of error functions. One possibility would be to use an error function which penalizes linearly the distance from the clipping intervals edges, see figure 5.3. Another possible error function would be a combination of the original one and the

Figure 5.3 Linearly Penalizing Error Function

linear penalizing error function, since extreme outliers could yield bad results for the position of the clipping window. See figure 5.4. This error function has already been

Figure 5.4 New Error Function

presented in the original work [20], but it has never been tested and applied. In [20], they also present a method, proposed by Attila Neumann, to calculate the clipping interval with the new error function in linear time:

The error weight at the position k is defined as $error(a, k)$ for the clipping interval $[a, b]$ where $b = a + CLIP$.

$$error(a,k) = \begin{cases} 0 & \text{for } k \in [a, b-1] \\ G & \text{for } k \in [1, a-d-1] \cup [b+d, k_{max}] \\ (a-k) \cdot \frac{G}{d+1} & \text{for } k \in [a-d, a-1] \\ (k-b) \cdot \frac{G}{d+1} & \text{for } k \in [b, b+d-1] \end{cases} \tag{5.8}$$

Let us say $g = \frac{G}{d+1}$ for given G and d.

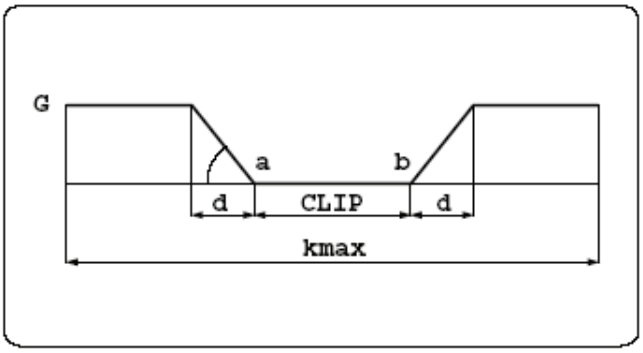

Figure 5.5 Error Function Details

We also need an additional pre-computed array, $e[a]$ which contains influences on the error for each step. It is defined recursively. First we need to define $f(a)$ as:

$$f(a) = \begin{cases} 0 & \text{for } a \leq 0 \\ f(a-1) + H[a] & \text{for } 1 \leq a \leq k_{max} \\ f(k_{max}) & \text{for } a > k_{max} \end{cases} \tag{5.9}$$

and $e[0]$ as:

$$e[0] = \sum_{i=1}^{k_{max}} error(0,i) = \sum_{CLIP+1}^{CLIP+d} (i - CLIP) \cdot G/d \cdot H[i] + G[f(k_{max}) - f(CLIP+d)] \tag{5.10}$$

The array element $e[0]$ corresponds to the first case and starting position, when you put the clippings interval starting point a over the first value in the histogram (at position l_{min}). Now we have to define $\Delta e[a+1]$ as:

$$\Delta e[a+1] = e[a+1] - e[a] \tag{5.11}$$

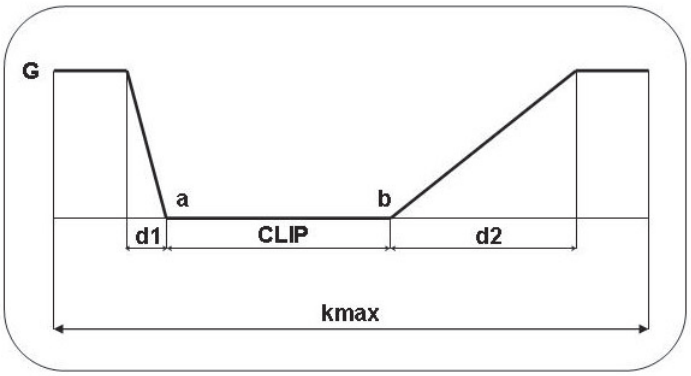

Figure 5.6 Alterable Penalties d1 and d2

then

$$e[a] = e[a-1]+g\cdot[f(a+1)-f(a-d)]-g\cdot[f(a+CLIP+d+1)-f(a+CLIP)] \quad (5.12)$$

After computing the array $e[a]$ we only need to find the minimal $e[a]$ for $a \in [0, k_{max} - CLIP]$ which is then the starting point of the clipping interval.

Alterable Penalties

As a further improvement, the penalty d can be switched into two linearly penalizing parts $d1$ and $d2$. It is an interesting question to define the optimal values for $d1$ and $d2$ in consideration to $CLIP$. In theory since the human eye does not discern very well in dark regions it would be appropriate to penalize more before the starting point A of the clipping interval as after the endpoint B hence $d1 < d2$. But typically if a scene has a big light source and a lot of information in the darker regions the better solution would be to take a bigger penalty in the “brighter zones” and a

smaller penalty in the "darker zones" of the histogram, hence $d1 > d2$. Realizing a lot of experiments this latter case was a significant better solution for arbitrary pictures (see chapter 6).

Chapter 6
Results

The pictures used in this work where partly taken by Professor László Neumann in Spain. The desk scene is a High Dynamic Range Image resulting of multiple Low Dynamic Range images created by Martin $\check{C}$adik. Also the other methods tested on the Desk scene -except the Minimal Information Loss Methods and the Mean Value Mapping- have been produced by Martin $\check{C}$adik.

On a 3GHz computer the algorithm performs in approximately 50 milliseconds over a 1 Megapixel image. The raw pictures used where unsigned integers for the pictures of László Neumann and float files for the HDRI pictures. Several different parameters where tested for the extended error function. Very good results were obtained with the parameters $D1 = 2 \cdot CLIP$ and $D2 = CLIP/5$. $L_{min} = 2^{-20}, L_{max} = 2^{20}, l_{min} = log2(L_{min}) = -20, l_{max} = log2(L_{max}) = 20; k_{max} = 8000, d = 0.005$ and $C = 45$ hence CLIP = 1098, D1 = 2196 and D2 = 220.

For the original Minimal Information Loss method we will give an amount of information loss in percent and for the extended version we will give a penalty value because it is not a 0-1 penalty where everything outside the clipping window is lost.

Chapel

Image size: 900 x 600

Figure 6.1 Original Picture from RAW generated with Matlab

Figure 6.2 Mean Value Mapping

Figure 6.3 Minimal Information Loss, Information Loss = 18%

Figure 6.4 Minimal Information Loss using MaxRGB, Information Loss = 8%

Figure 6.5 Minimal Information Loss with extended Error Function, Penalty Value = 26%

Figure 6.6 Minimal Information Loss with extended Error Function and MaxRGB, Penalty Value = 24%

On this picture taken by László Neumann, the minimal information loss with extended error function and MaxRGB yields a very good result where the true color of the wall on the right side is conserved even though the penalty value is 26% which is caused by the very big contrast in the image.

Granada

Image size = 600 x 900

Figure 6.7 Original Picture from RAW generated with Matlab

Figure 6.8 Mean Value Mapping

Figure 6.9 Minimal Information Loss Picture, Information Loss = 2.3%

As we can see here the mean value mapping burns out the floor and the blue of the sky is not blue anymore. The method only penalizes 2.3% of this high contrast scene.

The Desk

Image size = 2272 x 1704

Figure 6.10 Original Picture from RAW generated with Matlab

As we can see here the image has a very high contrast and even with the best value for linear tone mapping we get a penalty value of 29% which is still better then the approximate 50% we lose by using mean value mapping.

Figure 6.11 Minimal Information Loss, Information Loss = 30%

Figure 6.12 Minimal Information Loss with extended Error Function, Penalty Value = 30%

Figure 6.13 Minimal Information Loss with extended Error Function using MaxRGB, Penalty Value = 29%

Figure 6.14 Ward's Contrast Based Scale Factor

Figure 6.15 Drago et al. Logarithmic Mapping

Figure 6.16 Chiu et al. Tone Mapping Method

Figure 6.17 Fattal et al. Gradient Domain Model

Figure 6.18 Reinhard et al. Photographic Approach

Figure 6.19 Memorial Original Picture from RAW generated with Matlab

Figure 6.20 Minimal Information Loss with extended Error Function and MaxRGB, Penalty Value = 15%

Figure 6.21 Lamp Original Picture from RAW generated with Matlab

Figure 6.22 Minimal Information Loss with extended Error Function and MaxRGB

Figure 6.23 Belgium Original Picture from RAW generated with Matlab

Figure 6.24 Minimal Information Loss with extended Error Function and MaxRGB, Penalty Value 20%

Figure 6.25 Atrium Original Picture from RAW generated with Matlab

Figure 6.26 Minimal Information Loss, Information Loss = 4,4%

Figure 6.27 Minimal Information Loss with extended Error Function and MaxRGB, Penalty Value = 9%

Very low information loss for this high dynamic range image.

Chapter 7
Conclusion

In this work we presented a new approach to the Minimal Information Loss Method for Tone Mapping from 1998, introducing a new error-function and the MaxRGB function for contrast adjustment. This new method is easily understandable, fast, robust and efficient and can also be used for real time applications in computer animation like games etc. or in digital cameras instead of the Mean Value Mapping. Being a Global Tone Mapping Method, it does not aim to simulate the exact behavior of the Human Visual System with all it's perceptual effects etc. but it provides realistic and plausible pictures.

Although we get very good results with our test parameters, in the future more testing has to be done to define perfect default values for the Algorithm. The future work would also include to use a Gamut Mapping Method together with this Method to enhance the colors.

References

1. Alessandro Artusi, Real Time Tone Mapping, PhD Dissertation, Computergraphics Institute, Technical University of Vienna, 2004.

2. Ian Ashdown, Photometry and Radiometry, A Tour Guide for Computer Graphics Enthusiasts, 2002

3. M. Ashikhmin. A tone mapping algorithm for high contrast images. In 13th Eurographics Workshop on Rendering. Eurographics, June 2002.

4. H. R. Blackwell. Contrast Thresholds of Human Eye. Journal Opt. Soc. Am. 36, 11 (Nov.), pp. 624-643. 1946.

5. D. H. Brainard, D. G. Peli and T. Robson. Display Characterization. In Encyclopedia of Imaging Science and Technology. J. Hornak, (ed.), Wiley: 172-188. 2002

6. K. Chiu, M. Herf, P. Shirley, S. Swamy, C. Wang, and K. Zimmerman. Spatially nonuniform scaling functions for high contrast images. In Graphics Interface 93, pages 245253, Toronto, Ontario, Canada, May 1993. Canadian Information Processing Society.

7. K. Devlin, A. Chalmers, A. Wilkie, and W. Purgathofer. Tone Reproduction and Physically Based Spectral Rendering. Eurographics 2002: State of the Art Reports, Eurographics, 101–123, 2002.

8. Dowling, J. E. (1987). The Retina: An approachable part of the brain. Cambridge: Belknap.

9. F. Drago, K. Myszkowski, T. Annen, and N. Chiba. Adaptive Logarithmic Mapping For Displaying High Contrast Scenes. Eurographics EG 2003.

10. Fredo Durand and Julie Dorsey. Interactive tone mapping. In Rendering Techniques 2000: 11th Eurographics Workshop on Rendering, pages 219230. Eurographics, June 2000. ISBN 3-211-83535-0.

11. M. D. Fairchild. Colour Appearance Models. Addison Wesley, 1998.

12. M. D. Fairchild, and D. Wyble. Colorimetric Characterization of the Apple Studio Display (Flat Panel LCD). Munsell Color Science Lab., Rochester Institute of Technology, Rochester NY, Technical report, July 1998.

13. Raanan Fattal, Dani Lischinski, and Micheal Werman. Gradient domain high dynamic range compression. In Proceedings of ACM SIGGRAPH 2002, Computer Graphics Proceedings, Annual Conference Series. ACM Press / ACM SIGGRAPH, July 2002.

14. J. A. Ferwerda, S. N. Pattanaik, P. Shirley, and D. P. Greenberg. A Model of Visual Adaptation for Realistic Image Synthesis. ACM Computer Graphics (Proc. of SIGGRAPH)'96, pp. 249–258, 1996.

15. D. J. Jobson, Z. Rahman, and G. A. Woodell. A multiscale retinex for bridging the gap between color images and the human observation of scenes. IEEE Transactions on Image Processing, 6(7):965976, July 1997.

16. D. B. Judd, and G. Wyszecki Colour in Business, Science and Industry. John Wiley and Sons, 3nd Edition, 1975.

17. Grzegorz Krawczyk, Karol Krawczyk and Hans-Peter Seidel, Perceptual Effects in Real-Time Tone Mapping, ACM, Spring Conference on Computer Graphics 2005

18. Krešimir Matković, Tone Mapping Techniques and Color Image Difference in Global Illumination, PhD Dissertation, Computergraphics Institute, Technical University of Vienna, 1998.

19. G. Morvay, "New Photolexicon", Müszaki Könyvkiado, Budapest, Hungary, 1984.

20. L. Neumann and K. Matkovic and W. Purgathofer, Automatic Exposure in Computer Graphics Based on the Minimum Information Loss Principle, Proceedings of Computer Graphics International (CGI '98),IEEE Computer Society Press, pages 666-679, 1998

21. Laszlo Neumann, Kresimir Matkovic, Attila Neumann, Werner Purgathofer Incident Light Metering in Computer Graphics In Computer Graphics Forum 17(4), pp. 235-247, Blackwell, Oxford, December 1998.

22. S. N. Pattanaik, J. A. Ferwerda, M. Fairchild, and D. P. Greenberg. A Multiscale Model of Adaptation and Spatial Vision for Realistic Image Display. ACM Computer Graphics (Proc. of SIGGRAPH)'98, 287–298, 1998.

23. Sumanta N. Pattanaik, Jack E. Tumblin, Hector Yee, and Donald P. Greenberg. Time-dependent visual adaptation for realistic image display. In Proceedings of ACM SIGGRAPH 2000, Computer Graphics Proceedings, Annual Conference Series, pages 4754. ACM

24. C. A. Poyton. Gamma and its Disguises: The Nonlinear Mappings of Intensity in Perception, CRTs, Film and Video. SMPTE Jounal, pp. 1099-1108. December 1993.

25. Erik Reinhard, Michael Stark, Peter Shirley, and Jim Ferwerda. Photographic tone reproduction for digital images. In Proceedings of ACM SIGGRAPH 2002, Computer Graphics Proceedings, Annual Conference Series. ACM Press / ACM SIGGRAPH, July 2002.

26. A. Scheel, M. Stamminger, and Hans-Peter Seidel. Tone reproduction for interactive walkthroughs. Computer Graphics Forum, 19(3):301312, August 2000. ISSN 1067-7055.

27. C. Schlick. Quantization techniques for visualization of high dynamic range pictures. In 5th Eurographics Workshop on Rendering. Eurographics, June 1994.

28. G. Sharma. LCDs Versus CRTs Color Calibration and Gamut Considerations. Proceedings of the IEEE, Vol. 90, No. 4, April 2002.

29. SIGGRAPH 2004 Course #13 - "High Dynamic Range Imaging" Debevec, Reinhard, Ward, and Pattanaik, 2004

30. Greg Spencer, Peter S. Shirley, Kurt Zimmerman, and Donald P. Greenberg. Physically-based glare effects for digital images. In Proceedings of SIGGRAPH 95, Computer Graphics Proceedings, Annual Conference Series, pages 325334, Los Angeles, California, August 1995. ACM SIGGRAPH / Addison Wesley. ISBN 0-201- 84776-0.

31. L. Spillman, and J.S. Werner. Visual perception: the neurophysiological foundations. San Diego Accademic press 1990.

32. S. S. Stevens and J.C. Stevens, "Brightness Function: Parametric Effects of adaptation and contrast," Journal of the Optical Society of America, 53, 1139. 1960.

33. D. Travis. Effective Color Displays. Academic Press. 1990.

34. Tumblin J., Rushmeier H. 1993 Tone Reproduction for Realistic Images, IEEE Computer Graphics and Applications. 13(6), 42-48.

35. J. Tumblin, J. K. Hodgins, and B. K. Guenter. Two Methods for Display of High Contrast Images. ACM Transaction on Graphics, Vol. 18, No. 1, January 1999, pp. 56-94, 1999.

36. Jack Tumblin and Greg Turk. Lcis: A boundary hierarchy for detail-preserving contrast reduction. In Proceedings of SIGGRAPH 99, Computer Graphics Proceedings, Annual Conference Series, pages 8390, Los Angeles, California, August 1999. ACM SIGGRAPH / Addison Wesley Longman. ISBN 0-20148-560-5.

37. G. Ward, A Contrast-Based Scalefactor for Luminance Display, Graphics Gems IV, Ed. by P. S. Heckbert, pp. 415-421, 1994.

38. Ward G. and Shakespeare R, 1997, Rendering with Radiance: The Art and Science of Lighting Visualisation, Morgan Kaufmann Publication

39. G. Ward-Larson, H. Rushmeier, and C. Piatko. A Visibility Matching Tone Reproduction Operator for High Dynamic range Scene. IEEE Transaction on Visualization and Computer Graphics, Vol. 3 (4):291–306, 1997.

40. G. Wyszecki, and W. S. Stiles. Color Science: Concepts and Methods, Quantitative Data and Formulae. John Wiley and Sons, 2nd Edition, 1982.